



Tearing mode dynamics and sawtooth oscillations from CLT

Zhiwei Ma

Collaborators: W. Zhang and S. Wang

Institute of Fusion Theory and Simulation,
Zhejiang University, China

August 09, 2017, PPPL Seminar

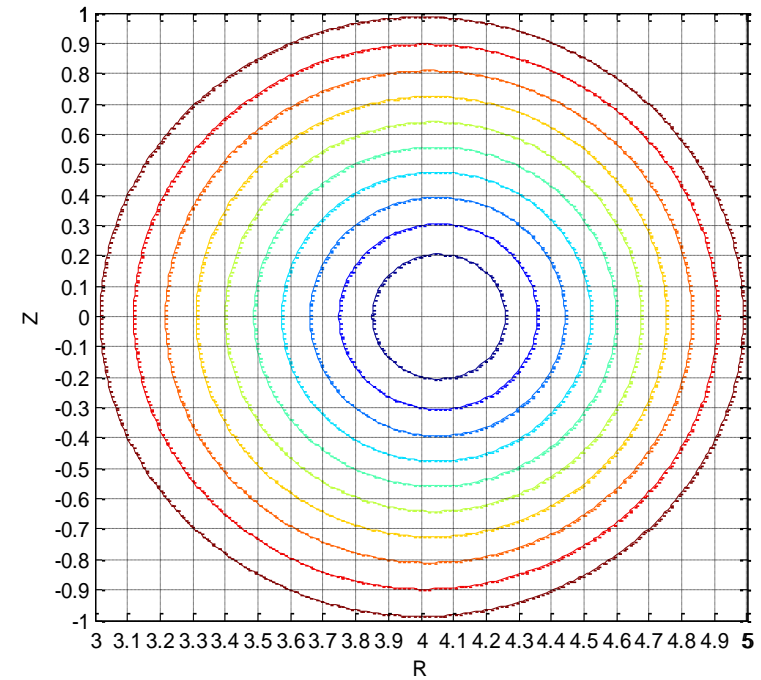
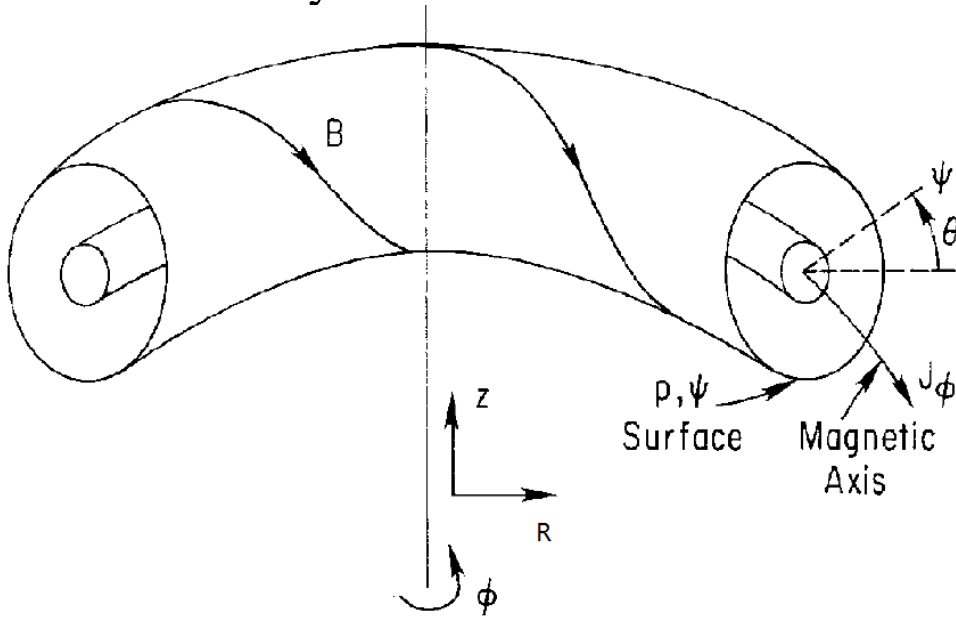
Outline

- **1. Brief introduction of CLT code**
- **2. TM controlled by driven current**
- **3. Hall effects on TM and DTM**
 - 2.1 Single tearing mode
 - 2.2 Double tearing mode
- **3. Hall effects on Sawtooth Oscillation**
- **4. Summary**

Development of Simulation Code

(CLT---Ci Liu Ti in chinese means MHD)

- For finite difference scheme:
- In the $(\psi[r], \theta, \phi)$ coordinate, the weakness is the singularity at $r=0$ and the small time step associated with $r^*d\theta$.
- In the (R, ϕ, Z) coordinated, the weakness is difficult to handle the boundary.



Hall MHD Equations:

$$\frac{\partial \rho}{\partial t} = -\nabla \cdot (\rho \mathbf{v}) + \nabla \cdot [D \nabla (\rho - \rho_0)]$$

$$\frac{\partial p_e}{\partial t} = -\mathbf{v} \cdot \nabla p - \Gamma p_e \nabla \cdot \mathbf{v} + \nabla \cdot [\kappa \nabla (p - p_0)]$$

$$\frac{\partial \mathbf{v}}{\partial t} = -\mathbf{v} \cdot \nabla \mathbf{v} + (\mathbf{J} \times \mathbf{B} - \nabla p_e) / \rho + \nabla \cdot [v \nabla (\mathbf{v} - \mathbf{v}_0)]$$

$$\frac{\partial \mathbf{B}}{\partial t} = -\nabla \times \mathbf{E}$$

$$\mathbf{E} = -\mathbf{v} \times \mathbf{B} + \eta (\mathbf{J} - \mathbf{J}_0) + \frac{1}{ne} (\mathbf{J} \times \mathbf{B} - \nabla P_e)$$

$$\mathbf{J} = \nabla \times \mathbf{B}$$

Numerical method

- In space, fourth order finite difference scheme in R and Z , finite difference scheme or pseudospectral scheme in ϕ .

$$\frac{\partial f_{i,j,k}}{\partial R} = \frac{f_{i+1,j,k} - f_{i-1,j,k}}{dR}$$

$$\frac{\partial^2 f_{i,j,k}}{\partial R^2} = \frac{f_{i+1,j,k} - 2f_{i,j,k} + f_{i-1,j,k}}{(dR)^2}$$

$$\frac{\partial f_{i,j,k}}{\partial Z} = \frac{f_{i,j+1,k} - f_{i,j-1,k}}{dZ}$$

$$\frac{\partial^2 f_{i,j,k}}{\partial Z^2} = \frac{f_{i,j+1,k} - 2f_{i,j,k} + f_{i,j-1,k}}{(dZ)^2}$$

$$\frac{\partial f_{i,j,k}}{\partial \phi} = \frac{f_{i,j,k+1} - f_{i,j,k-1}}{d\phi}$$

$$\frac{\partial^2 f_{i,j,k}}{\partial \phi^2} = \frac{f_{i,j,k+1} - 2f_{i,j,k} + f_{i,j,k-1}}{(d\phi)^2}$$

$$\frac{\partial \tilde{f}_{i,j,k}}{\partial \phi} = \frac{1}{2\pi} \sum_n [-i n \tilde{f}_{i,j}(n) e^{-in\phi}]$$

$$\frac{\partial^2 \tilde{f}_{i,j,k}}{\partial \phi^2} = \frac{1}{2\pi} \sum_n [-n^2 \tilde{f}_{i,j}(n) e^{-in\phi}]$$

$$\text{here } \tilde{f}_{i,j}(n) = \sum_k f_{i,j,k} e^{in\phi_k}$$

- In time, fourth-order Runge-Kutta method.

1.2 Benchmarks of CLT code

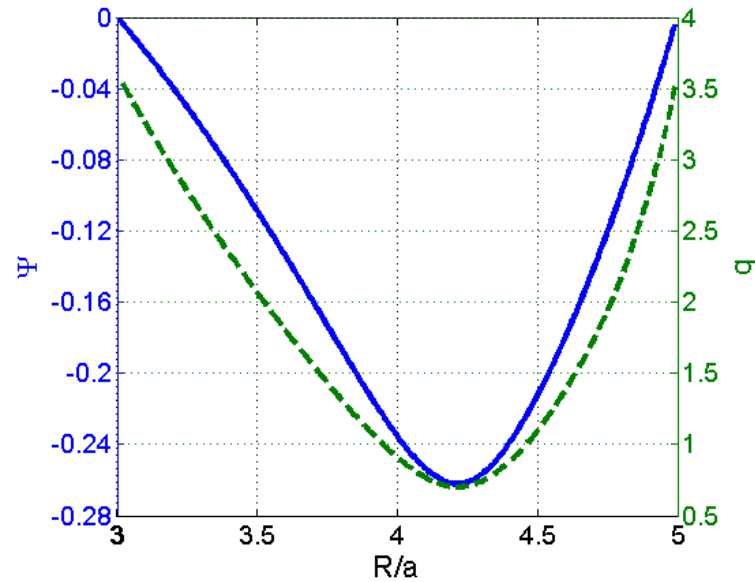
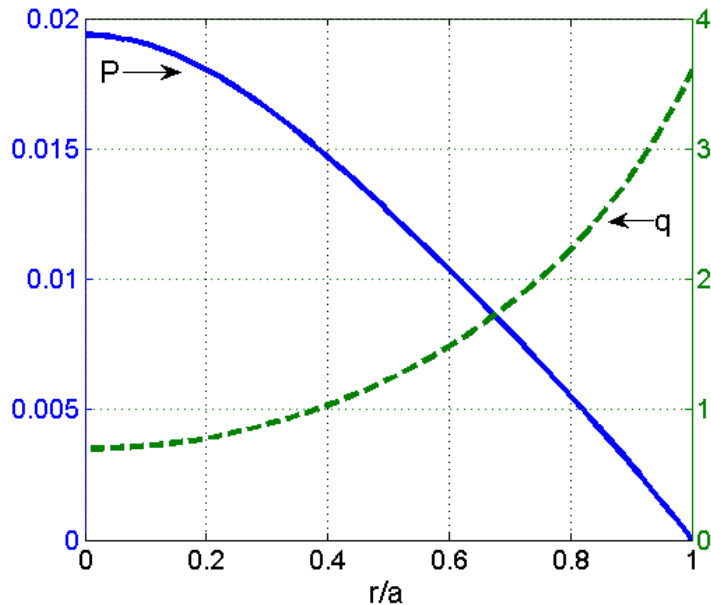
- A. Resistive kink mode($m/n=1/1$)
- B. Resistive tearing mode($m/n=2/1$)
- C. Double tearing mode($m/n=3/1$)

1. Resistive kink mode($m/n=1/1$)

- Equilibrium is obtained from NOVA code:

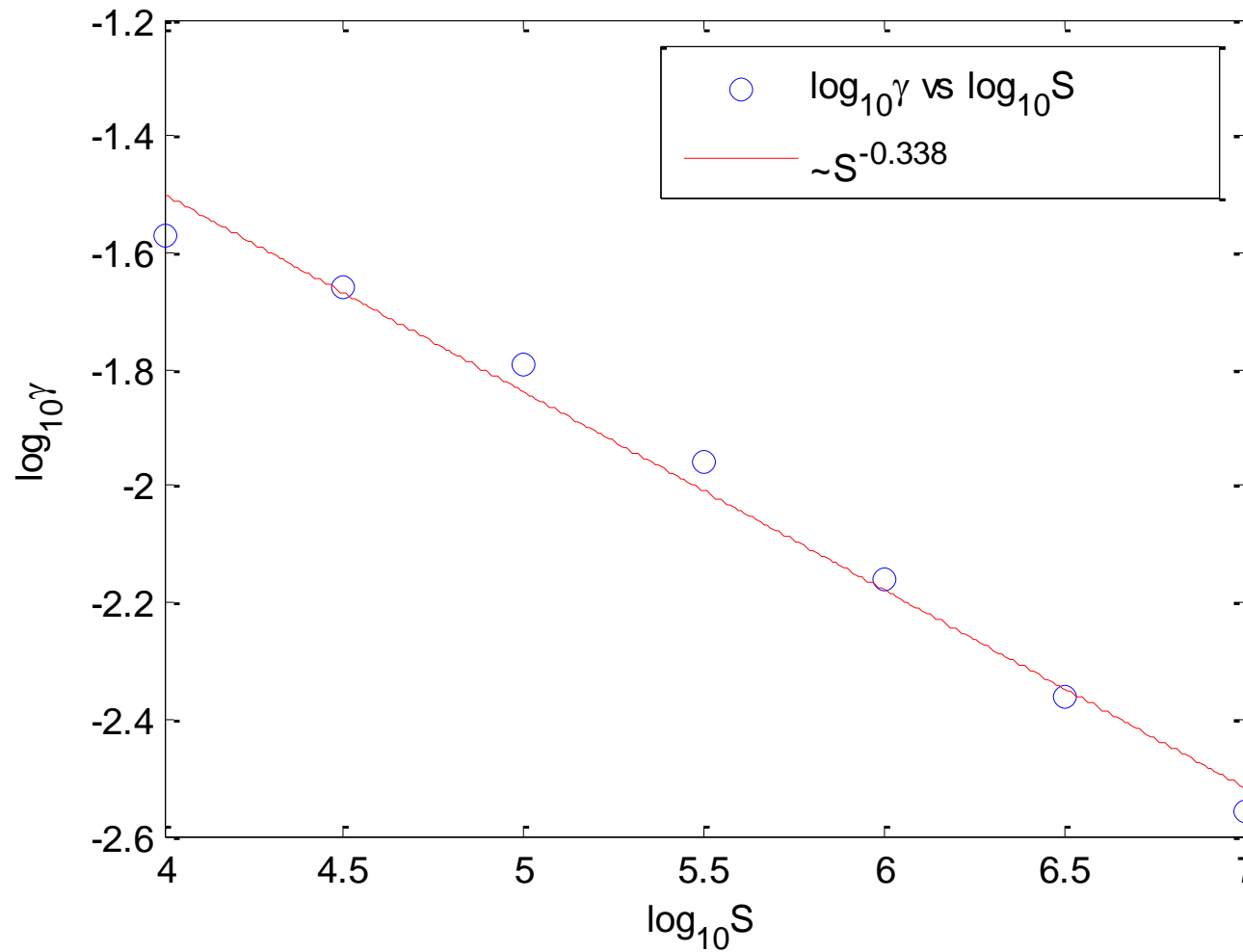
$\beta \sim 4.35\%$, $\rho_0 = 1$, $a = 1$, $R_0 = 4$, $q(0) = 0.73$, $q(a) = 3.6$,

The pressure and q profiles are given below:



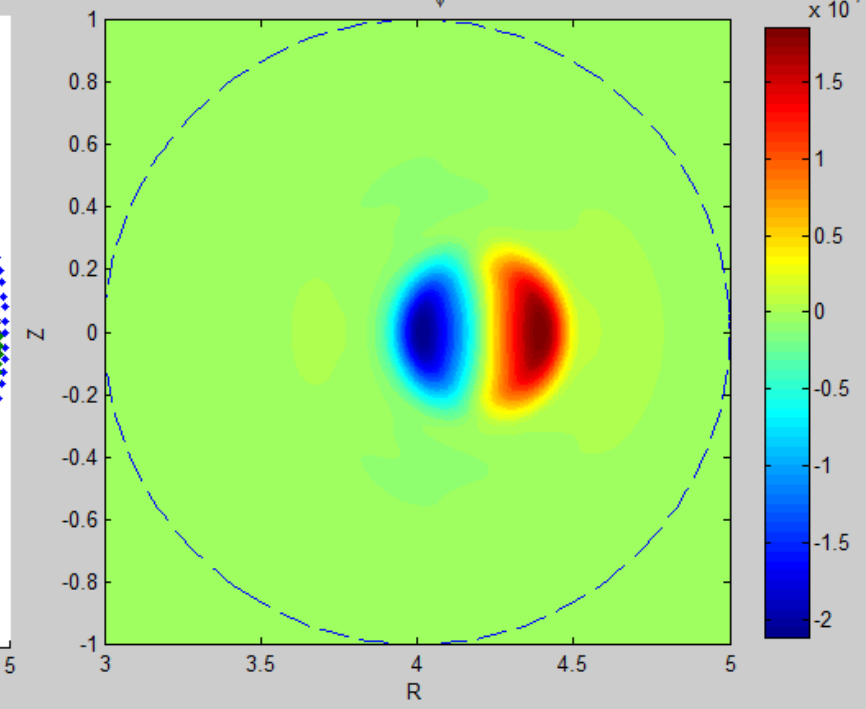
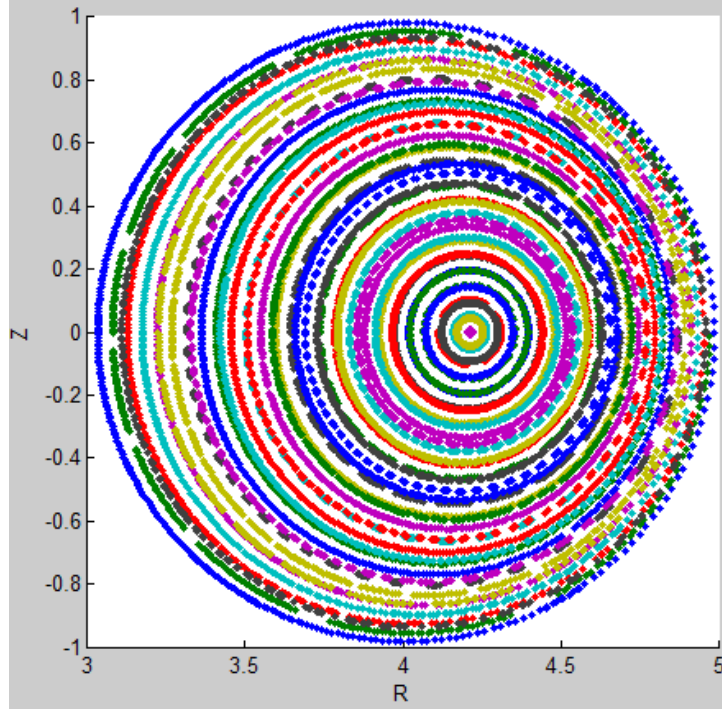
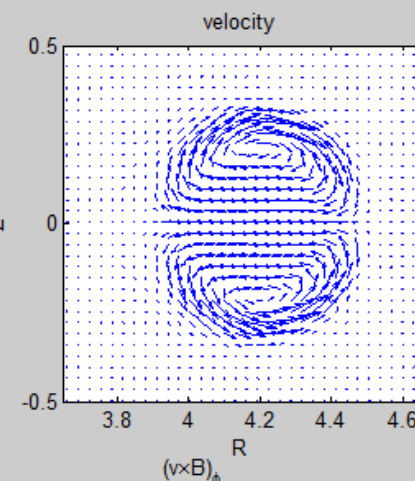
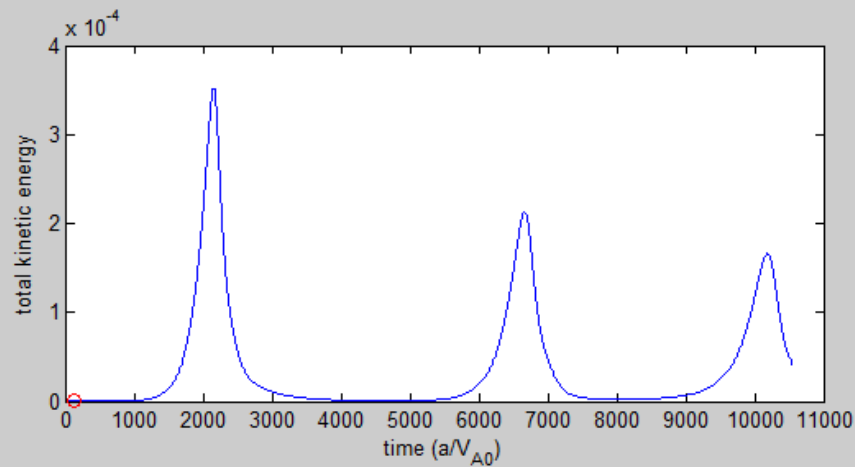
- Meshes: $mx=256$, $mz=256$, $my=32$

Linear growth rates vs S

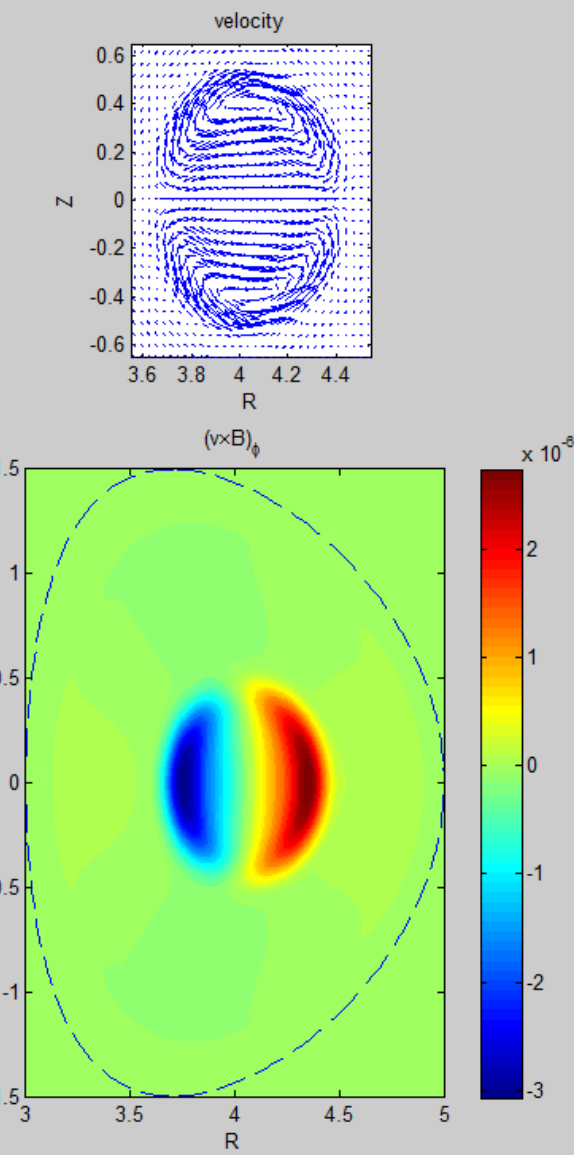
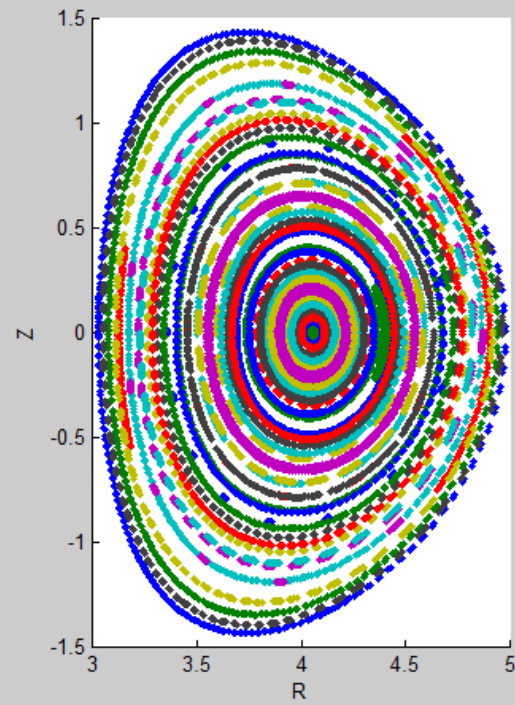
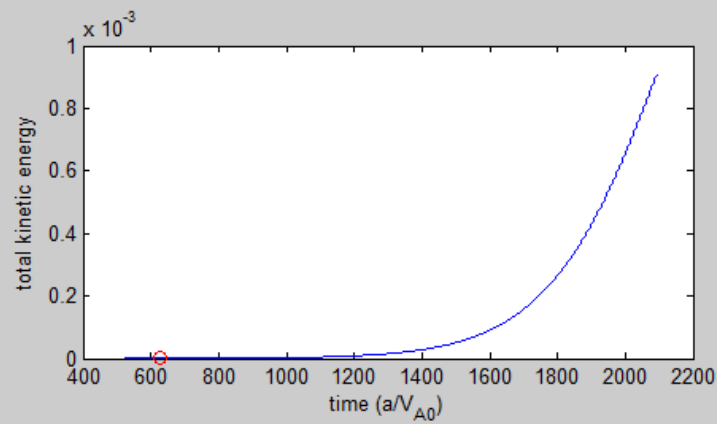


$n_0 = 2.5 \times 10^{-6}$, $t = 363.29$

$t = 105.73$ $\phi = 0$

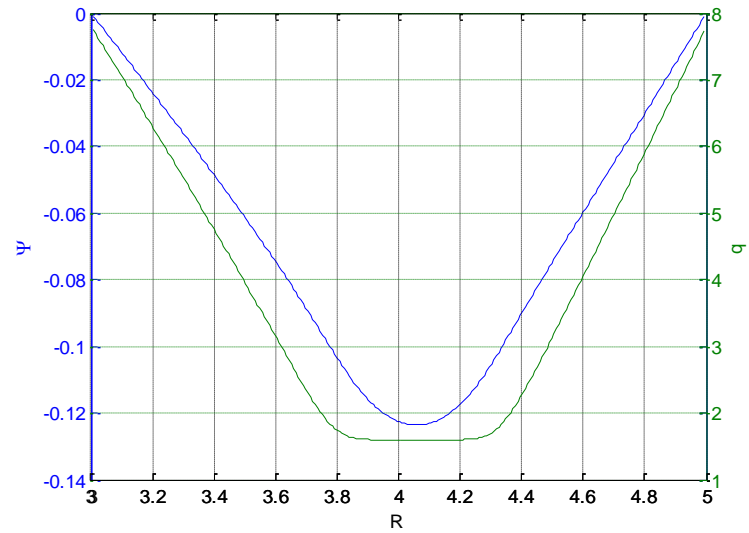
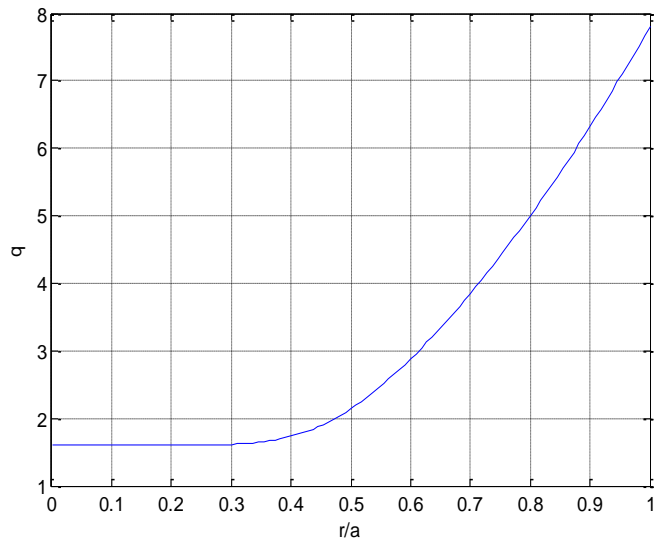


$t=628.27$ $\phi=0$

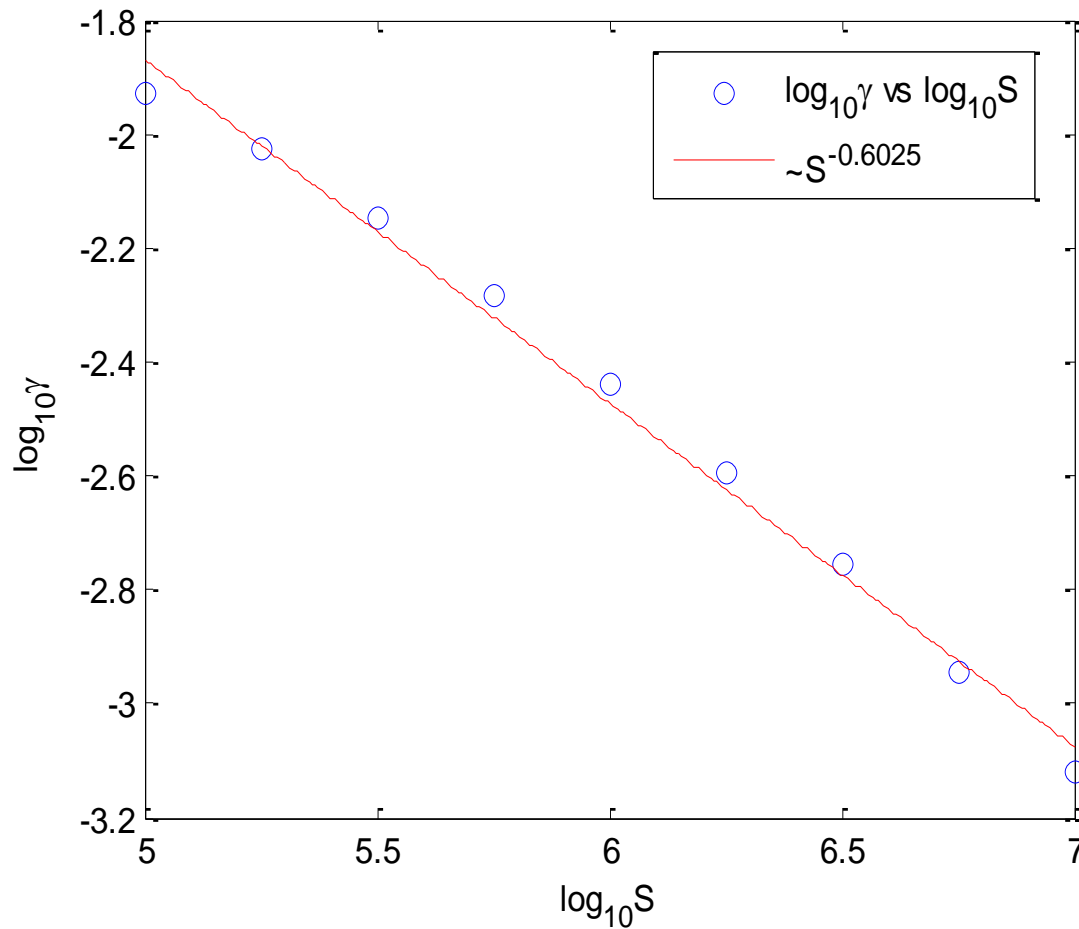


2. Resistive tearing mode($m/n=2/1$)

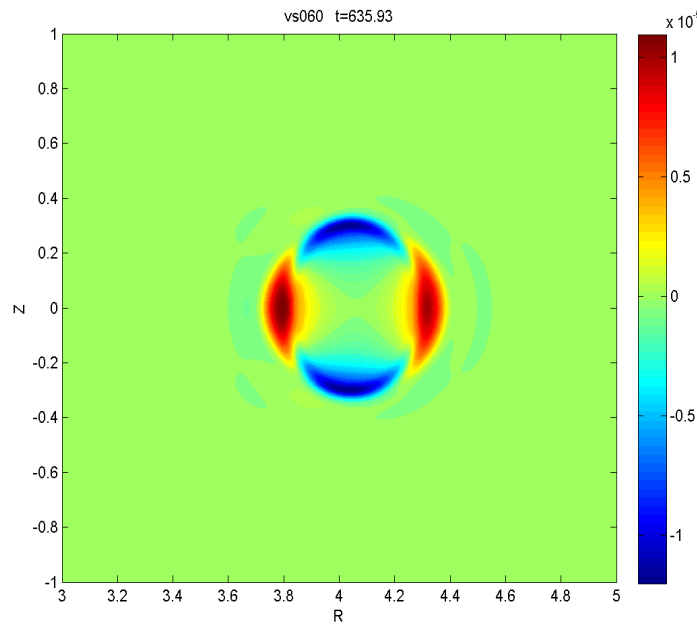
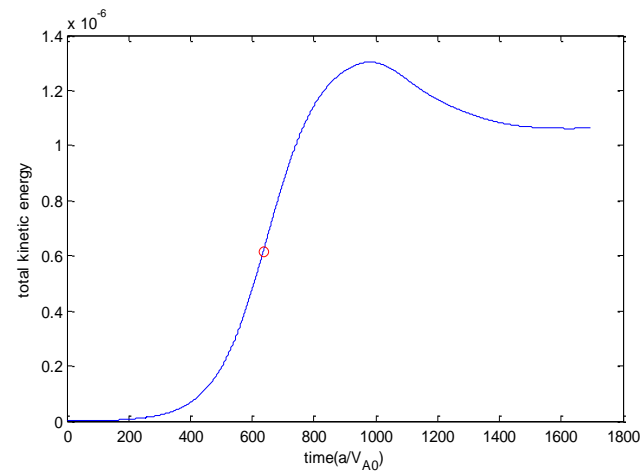
- $P_0 \sim 0$ ($\beta \sim 0$), $\rho_0 = 1$, $a = 1$, $R_0 = 4$, $q(0) = 1.6$, $q(a) = 7.8$,
- The q-profile is given as follows



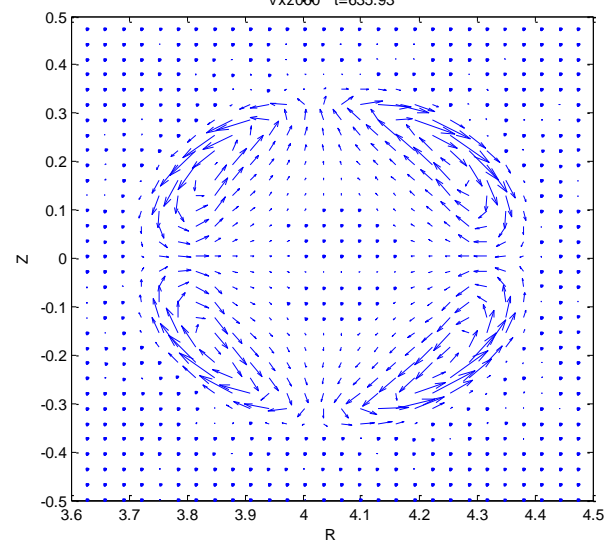
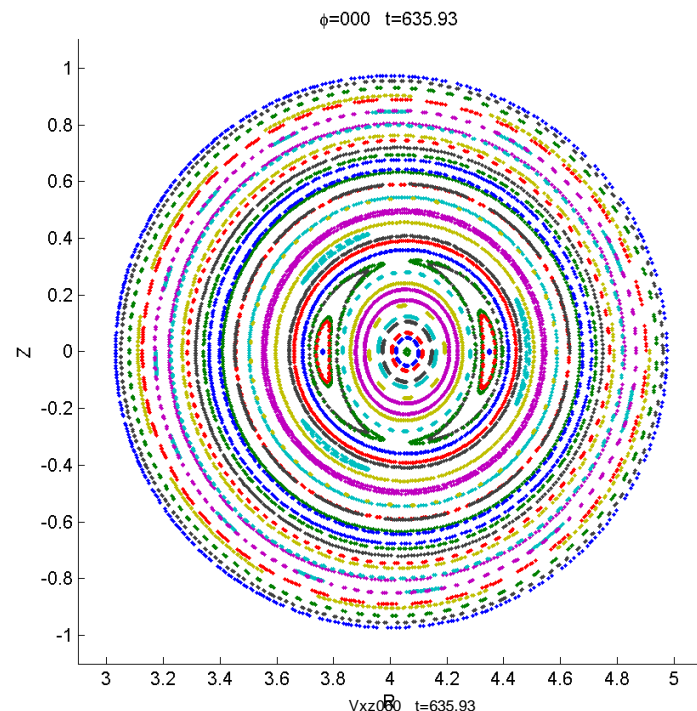
Linear growth rate vs S



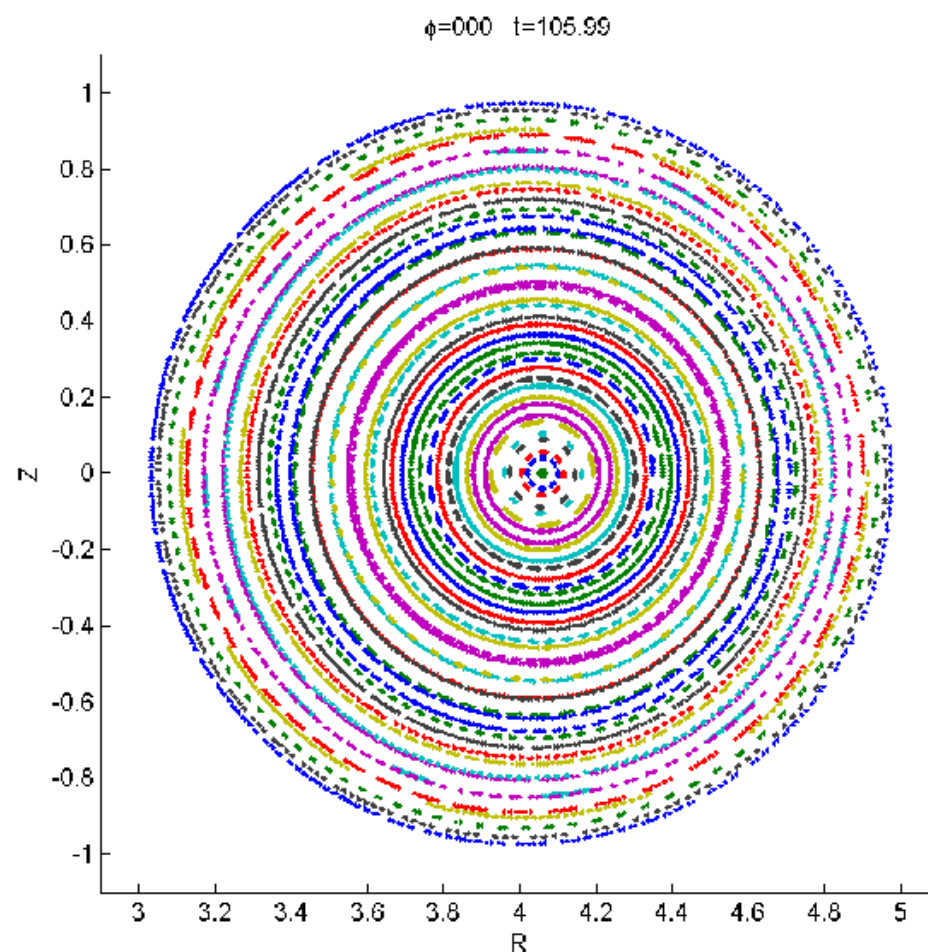
$$\eta_0=1 \times 10^{-5}, \quad t=635.93$$



$$\mathbf{v} \cdot \nabla \psi = (\mathbf{v} \times \mathbf{B})_\phi = v_Z B_R - v_R B_Z$$

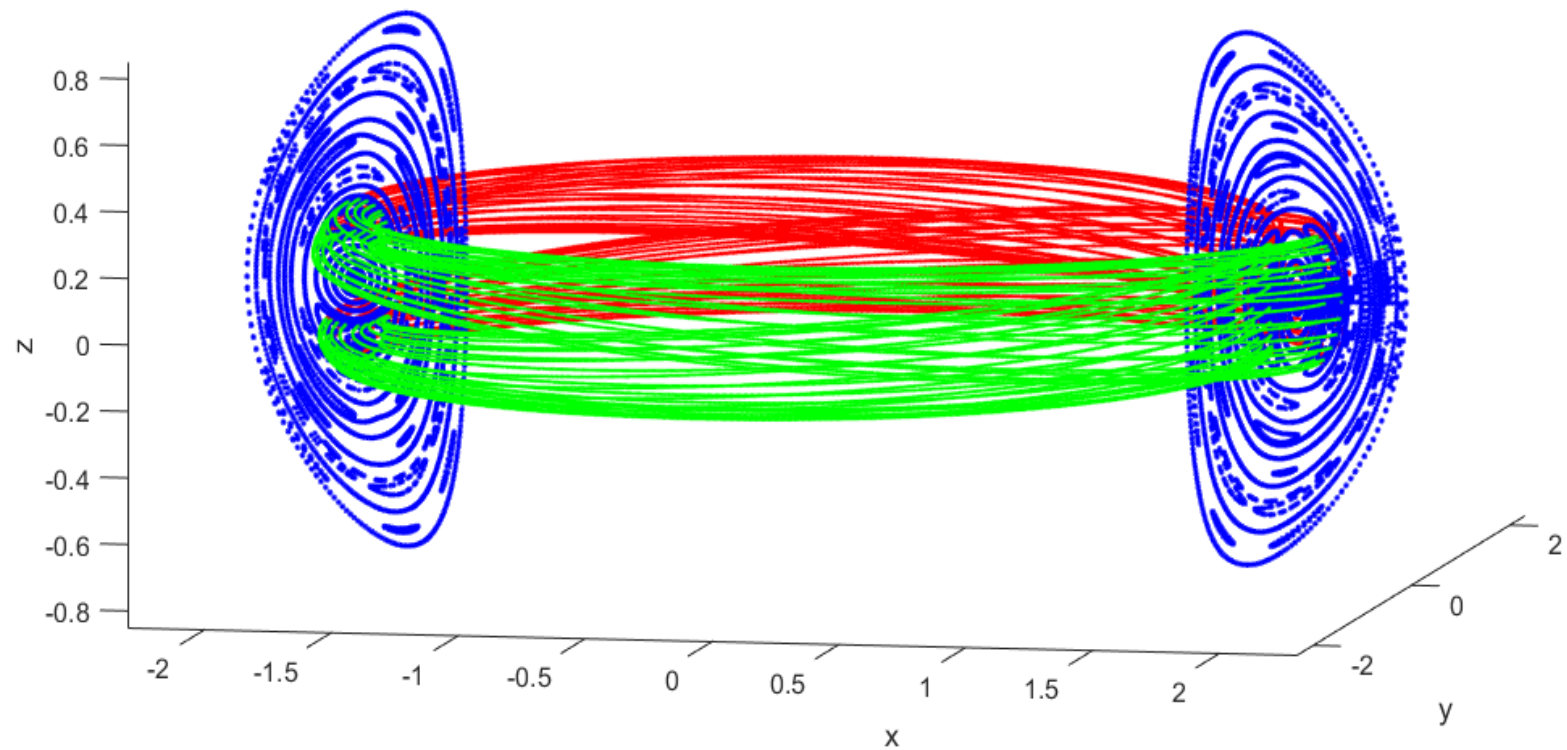


Time evolution of magnetic surfaces ($\eta_0=1\times10^{-5}$)



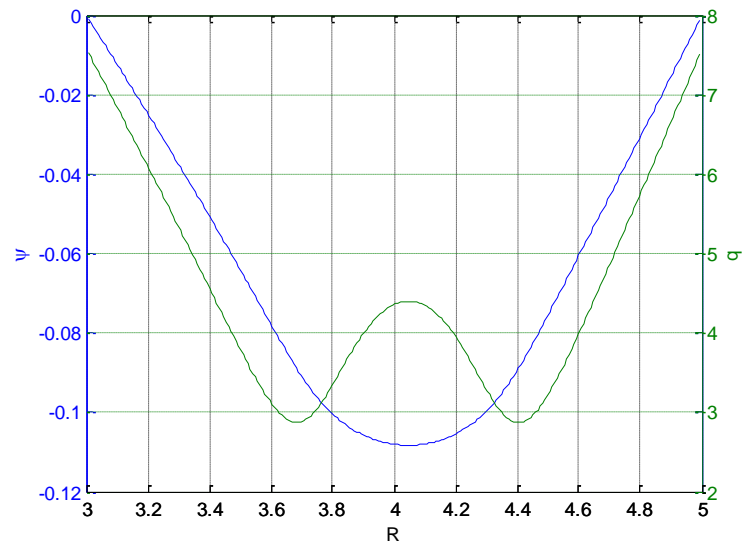
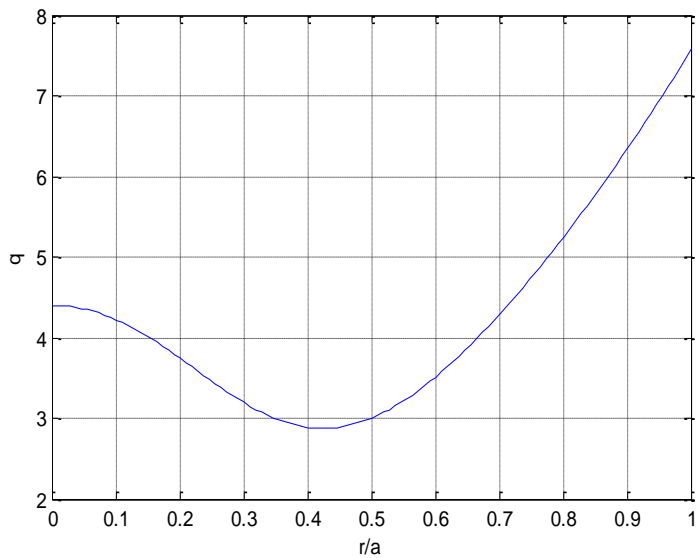
3D magnetic field lines and 2D magnetic surfaces

$t=5137.5$

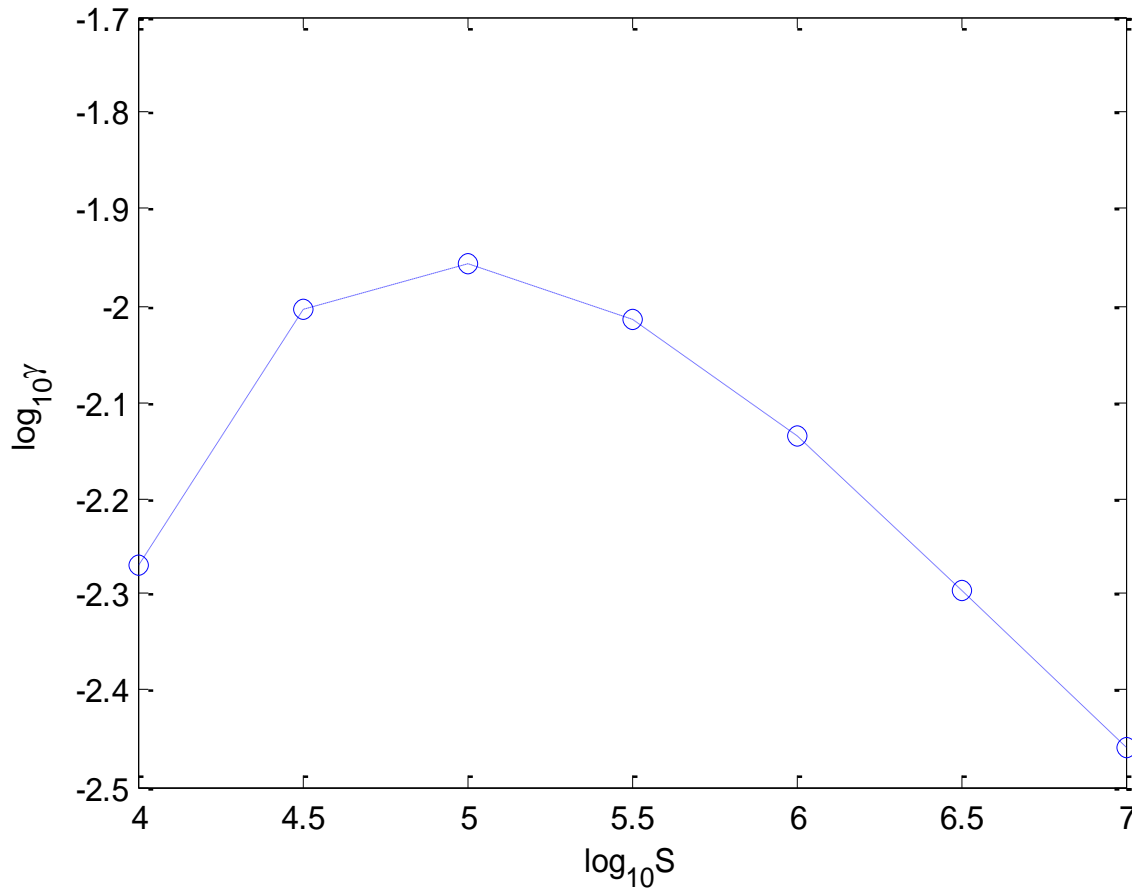


3. Double tearing mode($m/n=3/1$)

- $P_0 \sim 0$ ($\beta \sim 0$) , $\rho_0=1$, $a=1$, $R_0=4$,
- Current and q-profile are as follows:



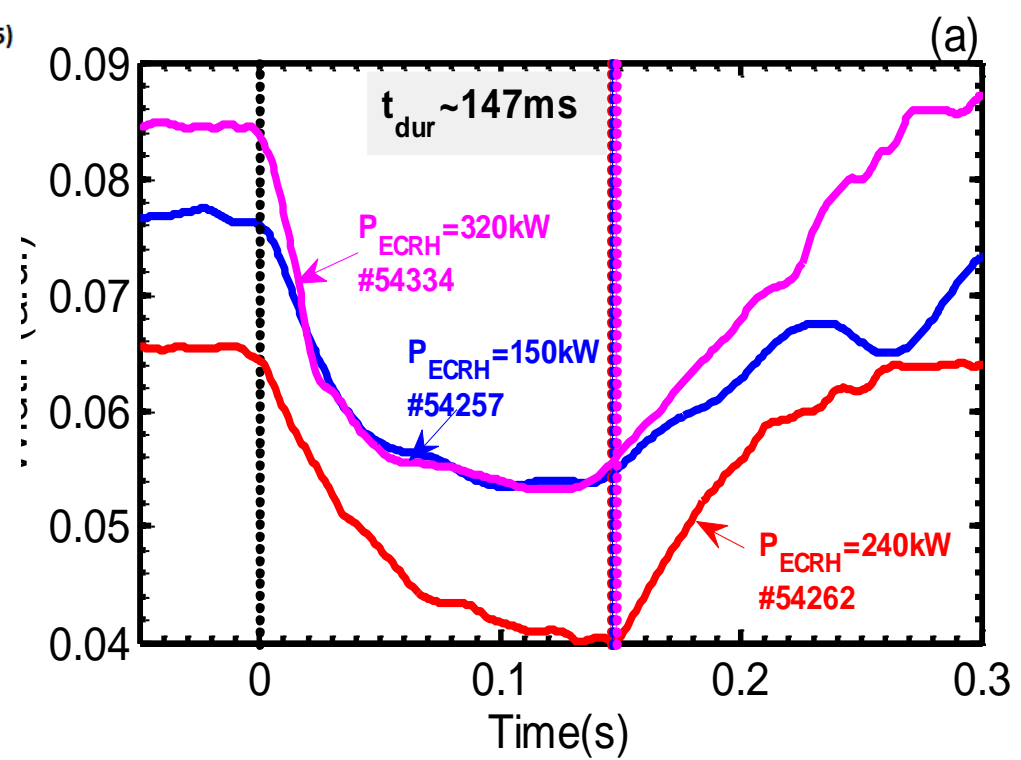
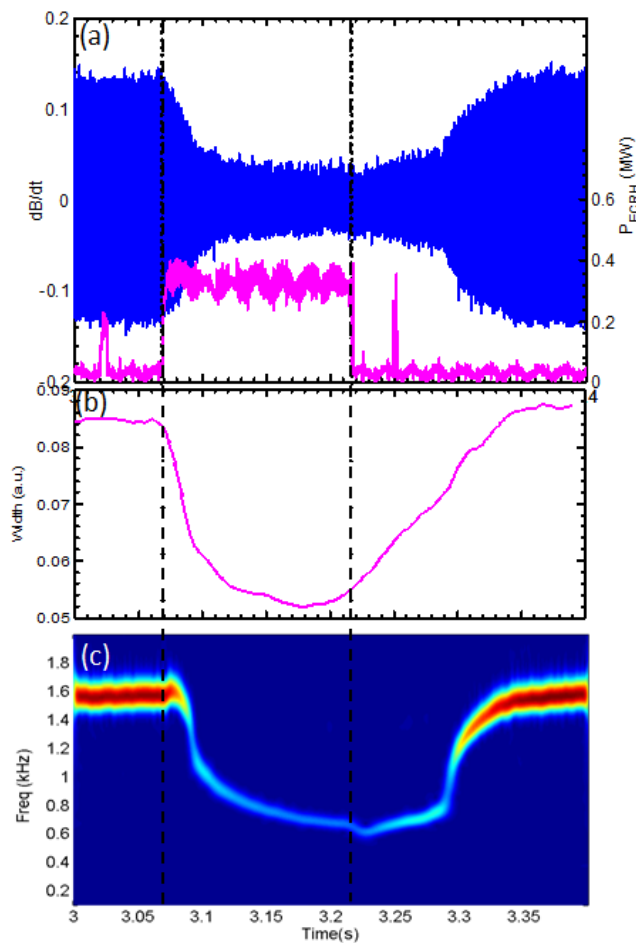
Linear growth rate vs S



2. *TM control by driven current*

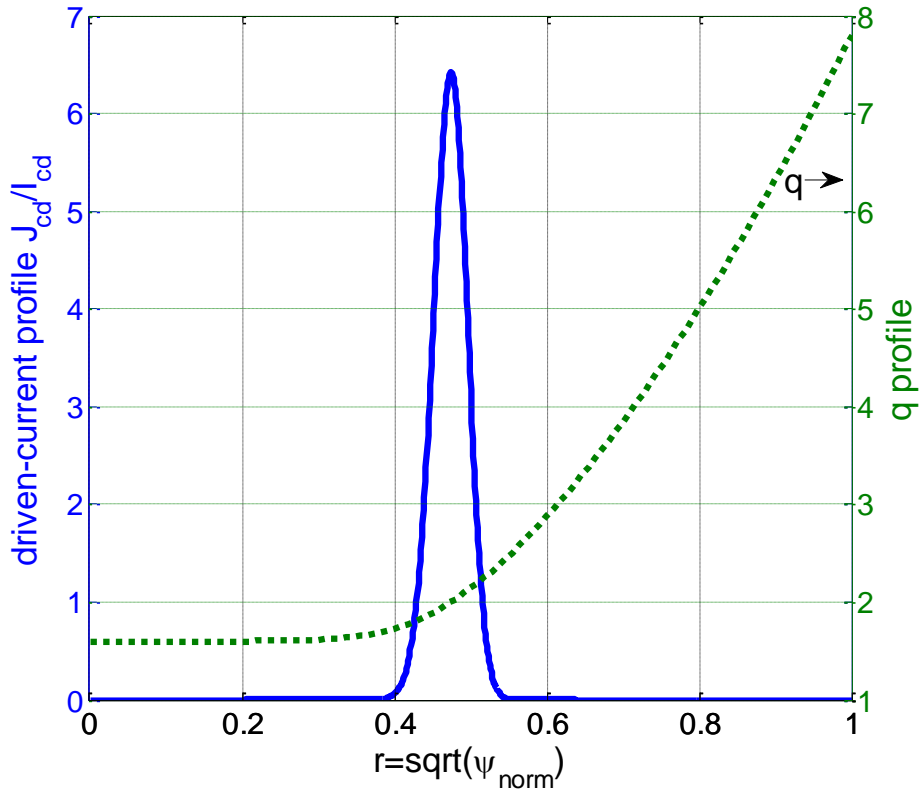
- EAST conducted some shots to investigate the tearing mode control by ECCD that is not published yet. With the power $P_{ECCD}=320\text{ kW}$, the equivalent driven current is $f_{cd} = 0.006$.

EAST #54334, EC beam injected with angle ($\phi=180^\circ$, $\theta=90^\circ$, $\rho_{dep}=0.5$)



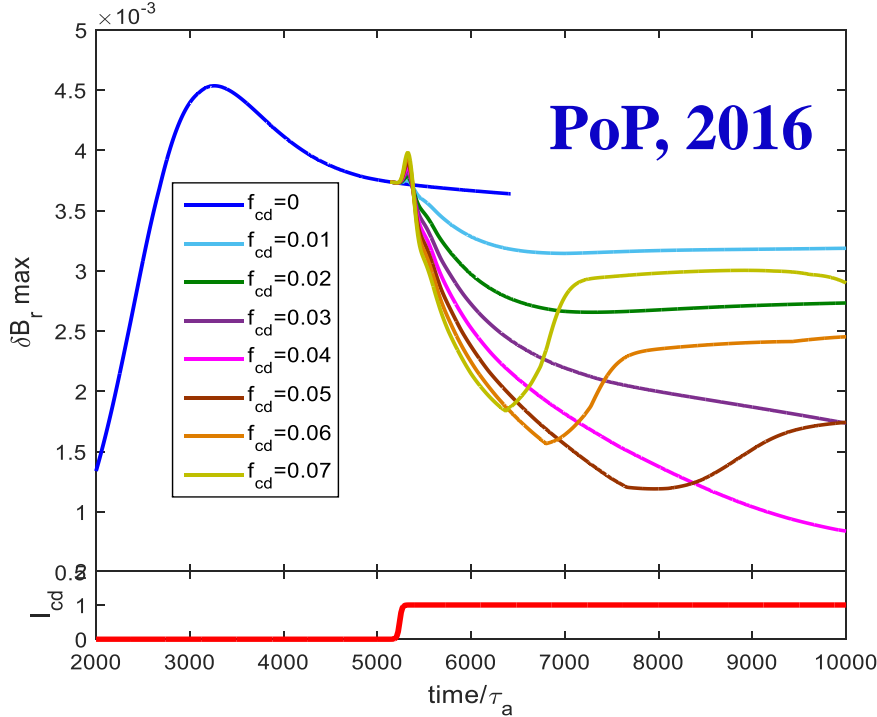
The size of the island is reduced about 35%.

- **EAST parameters:**
 - major radius $R_0=1.85\text{m}$,
 - minor radius $a=0.45\text{m}$,
 - elongation $E=1.9$,
 - triangle $\sigma =0.5$
 - resistivity $\eta=1.0*10^{-5}$,
 - viscosity $\nu=2.5*10^{-5}$,
 - diffusivity $D=1.0*10^{-4}$
 - low beta $\beta\sim 0$,
 - uniform density $\rho_0=1$,
 - q-profile as shown above
- The equilibrium plasma current $I_p(\text{MA})=0.26B_0(\text{T})$ under such condition.



Poloidally and toroidally uniform driven current

- Time evolutions of the amplitudes of perturbed radial magnetic field δB_r for various intensities of the driven current ($f_{cd}=0 - 0.07$)



$$J_{cd} = J_{cd0} e^{-\frac{(\psi - \psi_{cd})^2}{\delta_{cd}^2}}$$

$$\psi_{cd} = \psi_2 \equiv \psi(q_{eq}=2)$$

$$\delta_{cd} = 0.03$$

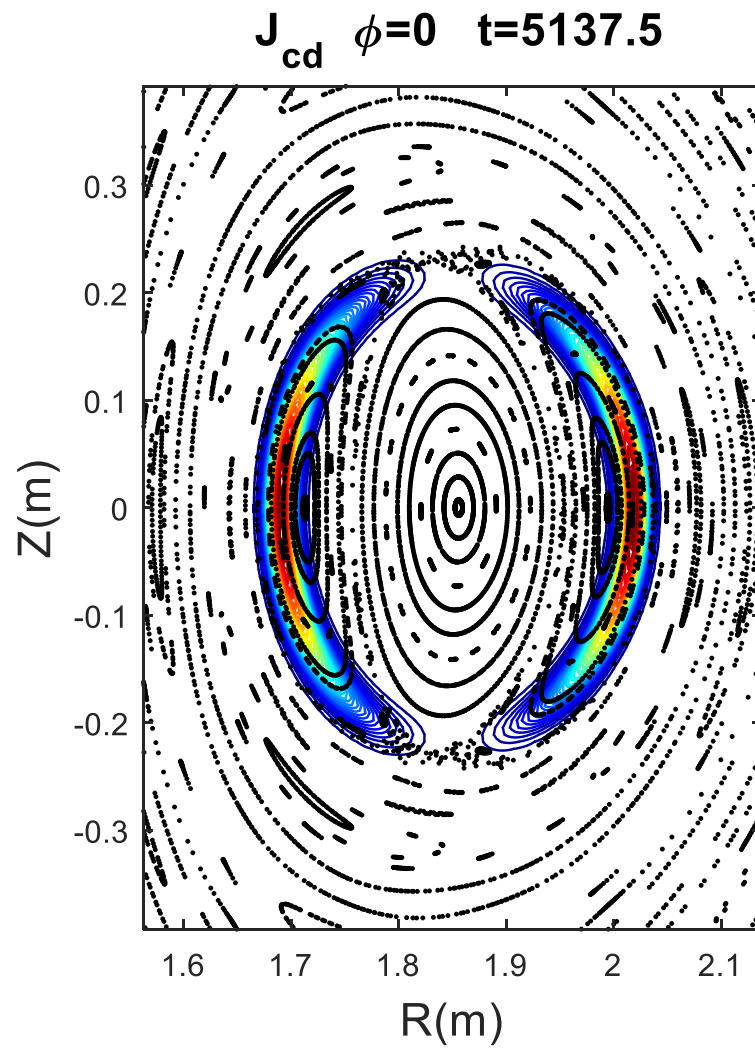
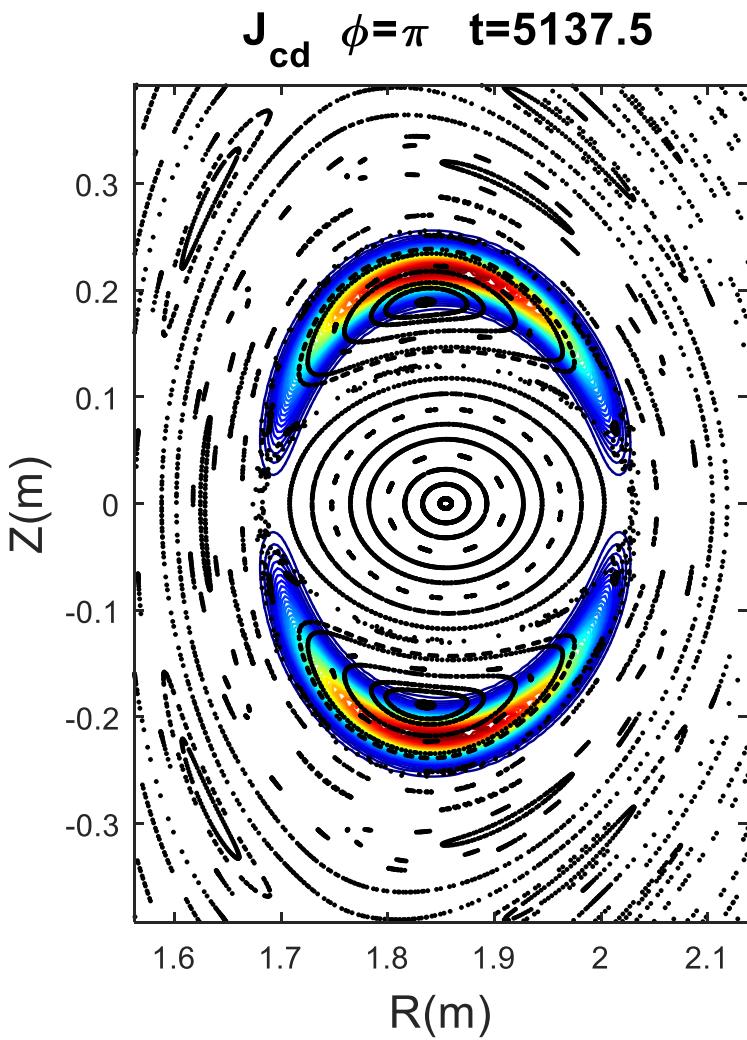
$$f_{cd} = I_{cd} / I_{eq} = 0.01 \sim 0.07$$

$$\Delta W \propto \sqrt{\delta B_r}$$

We have to impose the driven current to be
 $f_{cd} > 0.03$ for 35% reduction of island.

- $f_{cd} \leq 0.04$: the amplitude of the tearing mode decreases, and the final amplitude becomes smaller as stronger current drive, agreeing with Pletzer and Perkins, PoP (1999).
- $f_{cd} \geq 0.05$: the mode amplitude is rebounded after a period of decrease, and the final amplitude becomes larger as stronger current drive.

The driven current have to be helical
dependent due to fast motion of
electrons along magnetic field lines.



Helical dependent driven current

$$J_{cd}(\psi, \theta, \phi, t) = J_{cd0} e^{-\frac{(\psi - \psi_{cd}(t))^2}{\delta_{cd}^2}} [1 + \alpha(t) \cos(m(\theta - \theta_o(t)) + n\phi)]$$

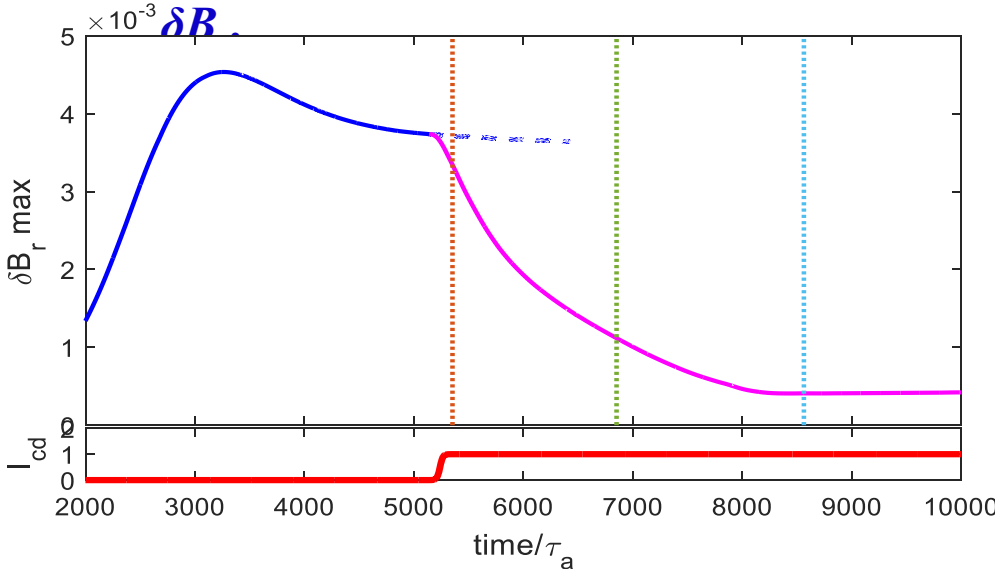
$$\psi_{cd}(t) = \frac{1}{2}(\psi_o + \psi_x) + \frac{1}{2}(\psi_o - \psi_x) \cos(m(\theta - \theta_o) + n\phi)$$

$$\alpha(t) = \frac{w(t)}{w_{sat}} \approx \left(\frac{\delta \bar{B}_r(t)}{\delta \bar{B}_{r,sat}} \right)^{1/2}$$

$\delta \bar{B}_r$: Amplitude of perturbed radial magnetic field (δB_r , max)
 $\delta \bar{B}_{r,sat}$: Amplitude of δB_r when the mode saturated (t=5137)

(ψ_o, θ_o) & (ψ_x, θ_x) : O-point & X-point of island found in $\varphi=0$ plane

- Time evolutions of the amplitudes of the perturbed radial magnetic field



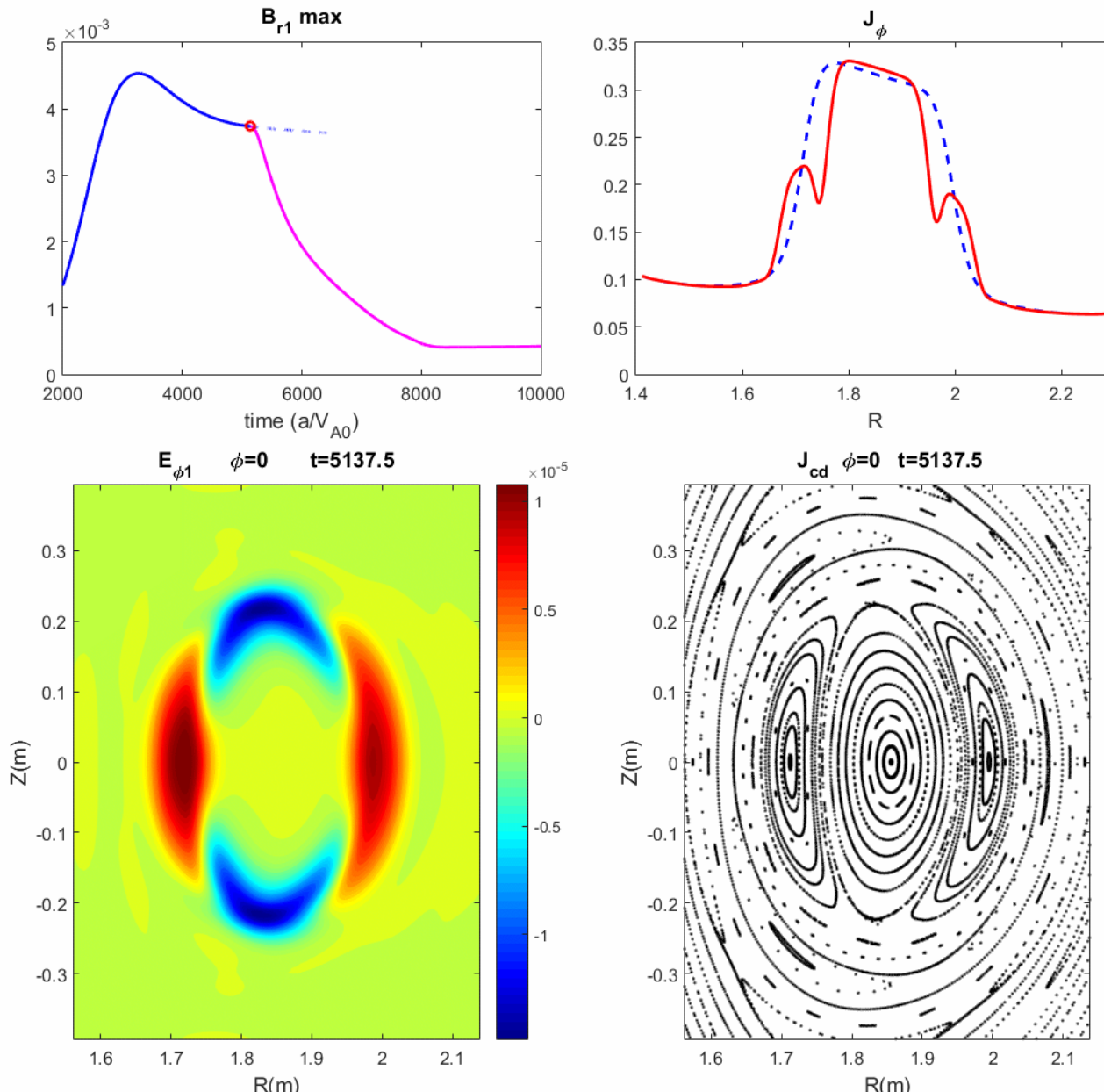
$$f_{cd} = 0.01$$

$$\delta_{cd} = 0.03$$

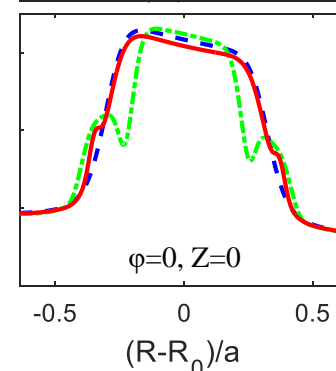
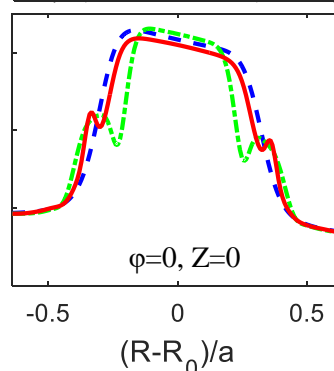
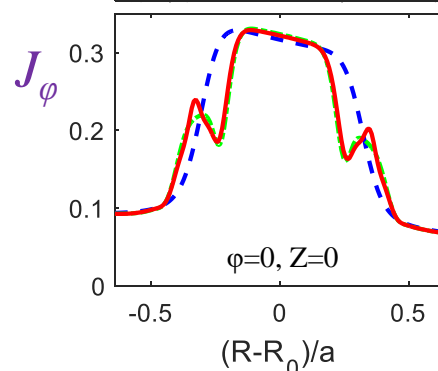
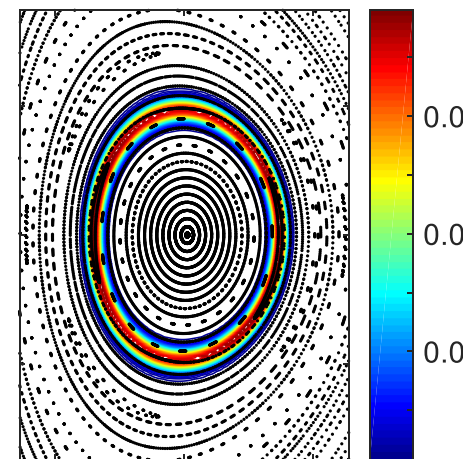
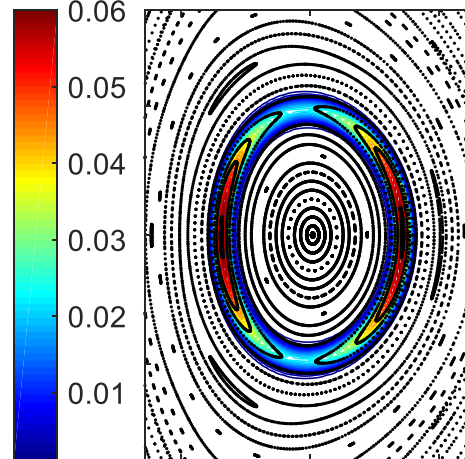
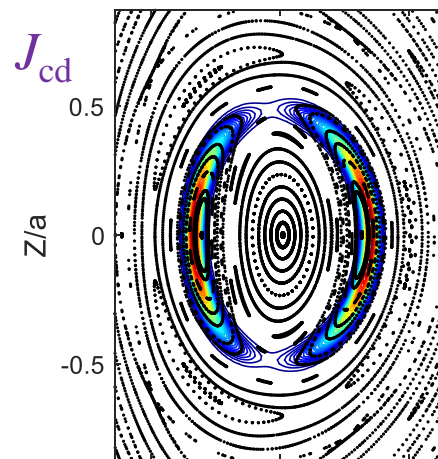
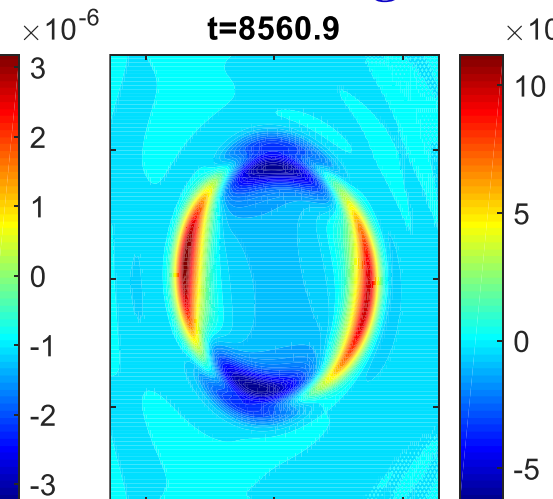
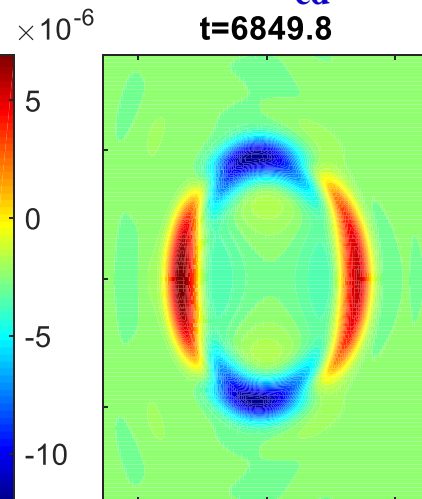
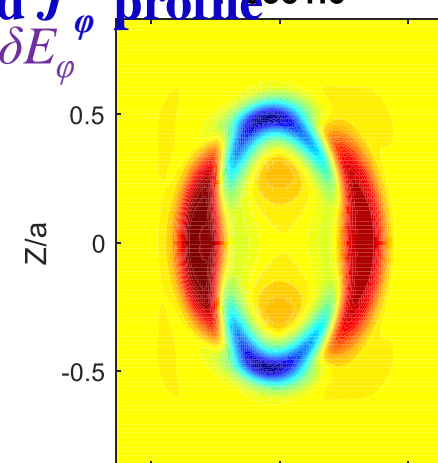
The result indicates that the island size can be reduced over 60% for the time dependent helical driven current with

$$f_{cd} = 0.01.$$

Driven current matching the island



Mode structures (δE_ϕ), driven current(J_{cd}) distributions with magnetic islands and J_ϕ profile



3. Hall effects on TM and DTM

Generalized Ohm's law (dimensionless form)

$$\mathbf{E} + \mathbf{v} \times \mathbf{B} = \frac{1}{S} \mathbf{J} + d_e^2 \frac{d\mathbf{J}}{dt} + \frac{d_i}{n} (\mathbf{J} \times \mathbf{B} - \beta_e \nabla p_e)$$

Δ_η $d_e \equiv L^{-1}(c / \omega_{pe})$ $d_i \equiv L^{-1}(c / \omega_{pi})$

Electron inertial length Ion inertial length

For the typical parameters in present Tokamak

$$n = 2 \sim 4 \times 10^{19} m^{-3}, \omega_{pi} = 0.6 \sim 0.8 \times 10^{10} s^{-1}$$

$$d_i = c / \omega_{pi} = 4 \sim 5 cm \quad d_i / a \sim 0.1 \quad \Delta_\eta / a = 10^{-3} \sim 10^{-4}$$

The current sheet thickness Δ_η will goes down below ion inertial length, i.e.,

$$\Delta_\eta \ll c / \omega_{pi}$$

Hall term in the generalized Ohm's law cannot be ignored.

1.1 Hall effect

- Hall effect will play two important roles on dynamics of tearing mode: diamagnetic rotation and fast development in the nonlinear stage.
- Both ion and electron pressure gradients in a Tokamak lead to diamagnetic rotation with the frequencies.

$$\omega_{*i,e} = \pm \frac{1}{en_0 r B_{t0}} \frac{dp_{i,e}}{dr}$$

- Due to the large mass ratio,
 - Ion pressure gradient \rightarrow plasma flow;
 - electron pressure gradient \rightarrow rotation of the magnetic field perturbation due to the frozen-in condition.

- Because of cold ion assumption in Hall MHD,
 - Diamagnetic rotation of the mode structure,;
 - No plasma rotation flow
- In previous simulations Xtor-2F, the diamagnetic flow as an initial background flow is added into the momentum equation to study diamagnetic rotation effects on the tearing mode instability

$$\frac{\partial \mathbf{v}}{\partial t} = -\mathbf{v} \cdot \nabla \mathbf{v} - \mathbf{v}_* \cdot \nabla \mathbf{v} + (\mathbf{J} \times \mathbf{B} - \nabla p) / \rho$$

- Current sheet is collapsed due the decoupling of the ion and electron motion, which gives rise to fast development of the tearing mode in the nonlinear stage.

CLT Upgrade

$$\frac{\partial \rho}{\partial t} = -\nabla \cdot (\rho \mathbf{v}) + \nabla \cdot [D \nabla (\rho - \rho_0)]$$

$$\frac{\partial p_e}{\partial t} = -\mathbf{v} \cdot \nabla p - \Gamma p_e \nabla \cdot \mathbf{v} + \nabla \cdot [\kappa \nabla (p - p_0)]$$

$$\frac{\partial \mathbf{v}}{\partial t} = -\mathbf{v} \cdot \nabla \mathbf{v} + (\mathbf{J} \times \mathbf{B} - \nabla p_e) / \rho + \nabla \cdot [\mathcal{W}(\mathbf{v} - \mathbf{v}_0)]$$

$$\frac{\partial \mathbf{B}}{\partial t} = -\nabla \times \mathbf{E}$$

Hall term

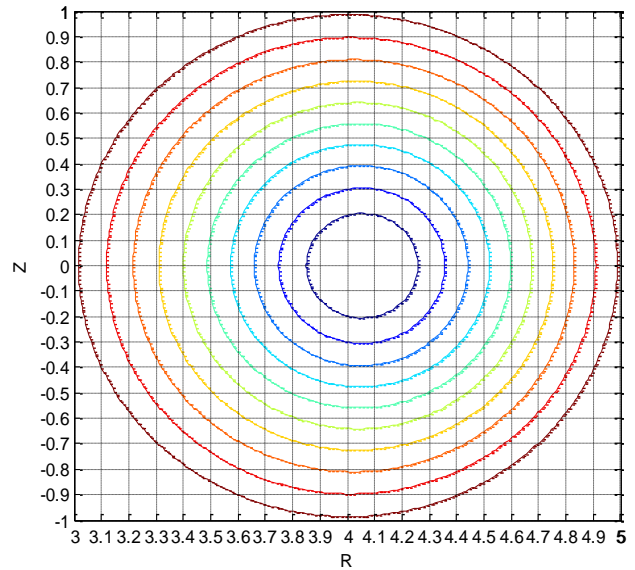
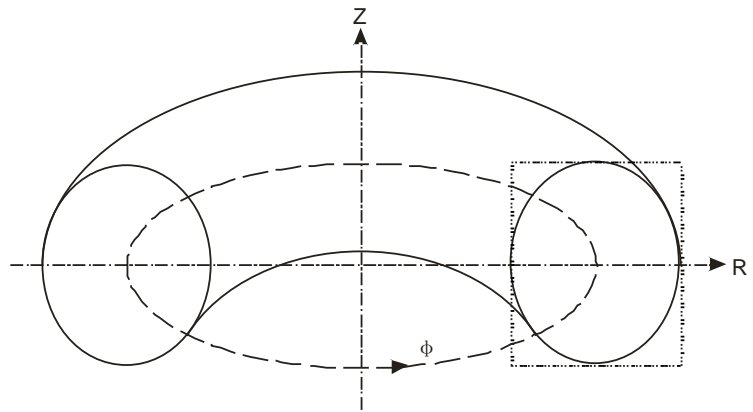
$$\mathbf{E} = -\mathbf{v} \times \mathbf{B} + \eta(\mathbf{J} - \mathbf{J}_0) + \frac{1}{ne}(\mathbf{J} \times \mathbf{B} - \nabla P_e)$$

$$\mathbf{J} = \nabla \times \mathbf{B}$$

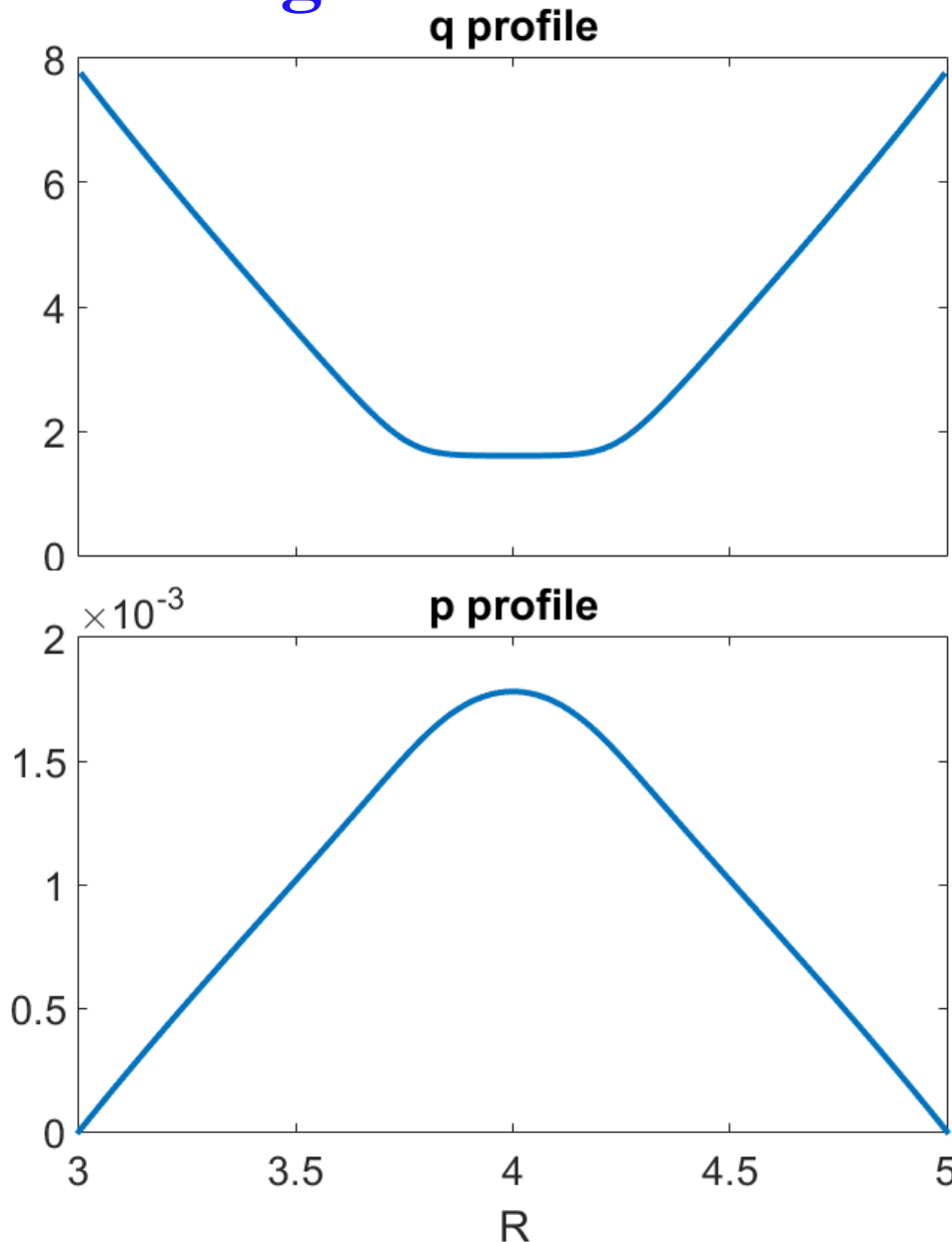
In previous studies Xtor-2F, they use:

$$\mathbf{E} = -\mathbf{v} \times \mathbf{B} + \eta(\mathbf{J} - \mathbf{J}_0) + \frac{1}{ne} \nabla_{||} P_e$$

$$\mathbf{v} \cdot \nabla \mathbf{v} \rightarrow (\mathbf{v} + \mathbf{v}_{i*}) \cdot \nabla \mathbf{v}$$



3.1. Single TM: Rotation of mode structure



Asssuming $\gamma \gg \omega_{e^*}$

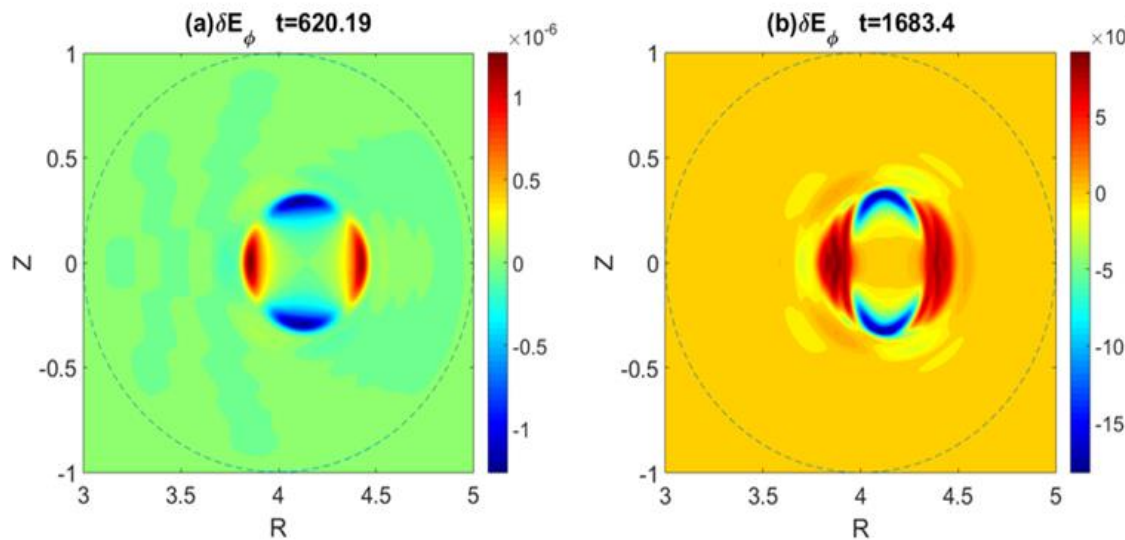
$$\gamma \approx \gamma_0 \left(1 - \frac{2}{25} \frac{\omega_{e^*}^2}{\gamma_0^2}\right)$$

$$\omega = -\frac{4}{5} \frac{m}{nerB_0} \frac{dP}{dr} = \frac{4}{5} m \omega_{e^*}$$

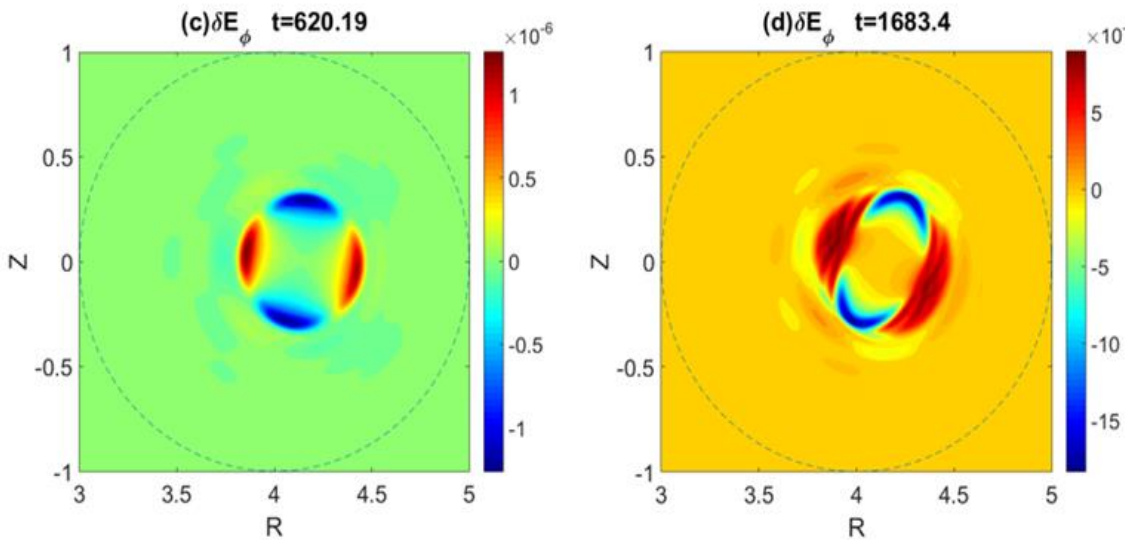
$$\omega_{e^*} = -\frac{1}{nerB_0} \frac{dp}{dr}$$

Simulation results from CLT

MHD



Hall
MHD



Simulation:

$$T_* \approx 2.00 \times 10^4 t_A$$

Theory:

$$T_* \approx 2.07 \times 10^4 t_A$$

Rotation frequency due to Hall effect: $\omega = 4m\omega_* / 5$

Linear growth rates with Hall effect

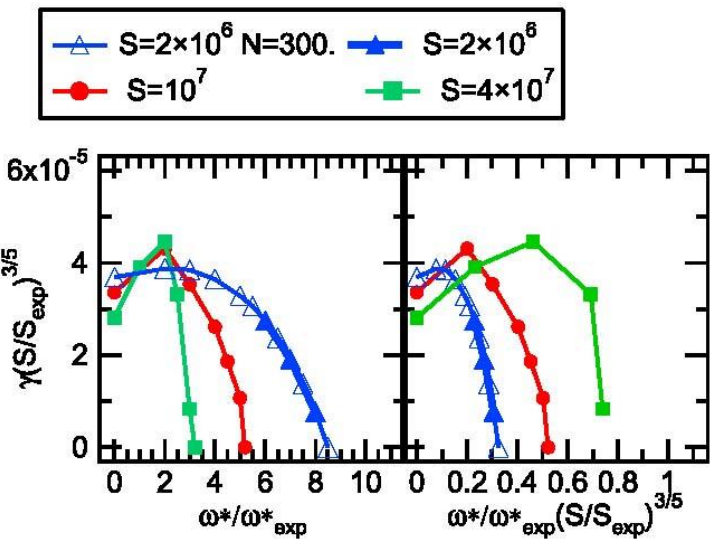
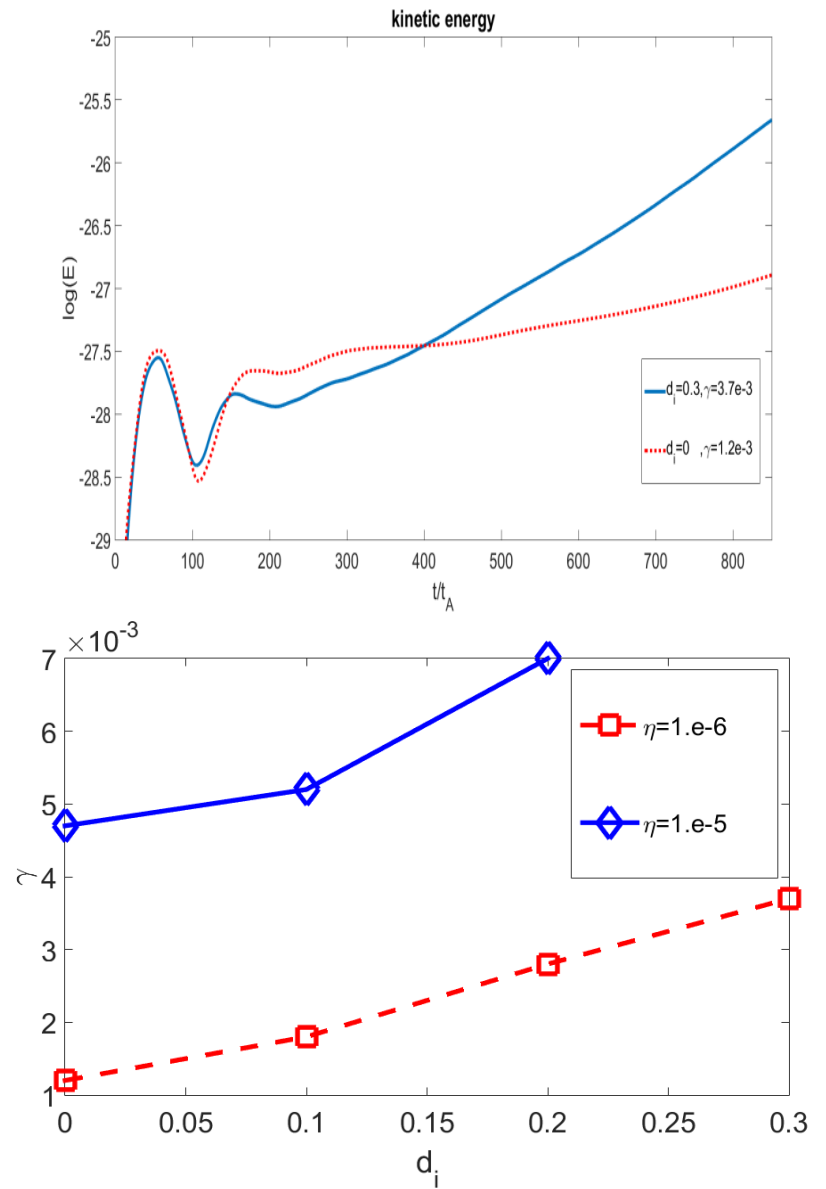
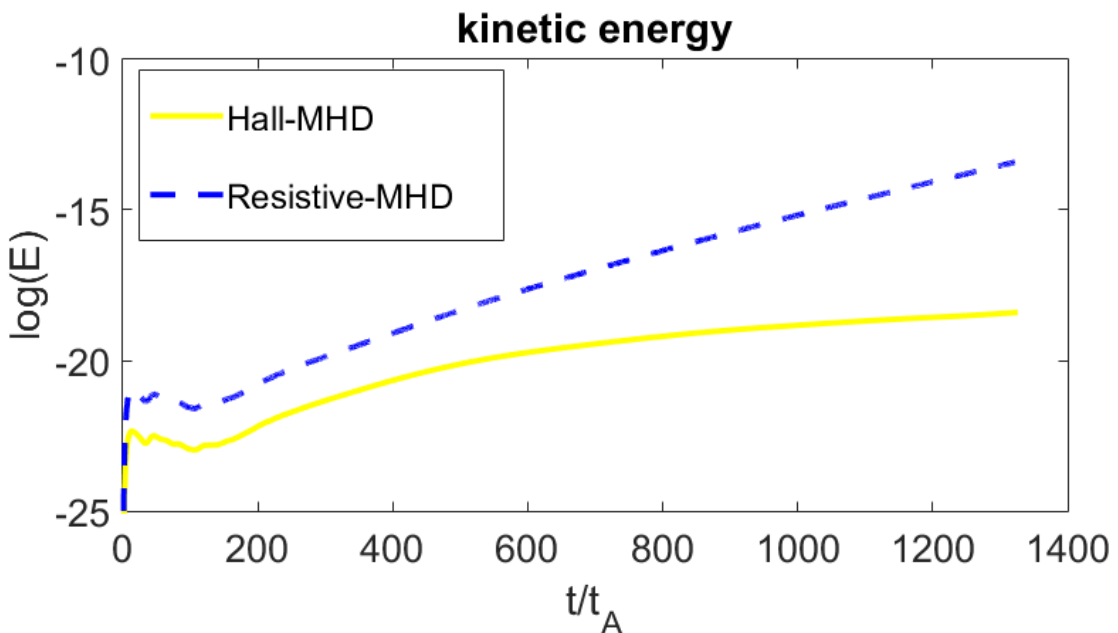
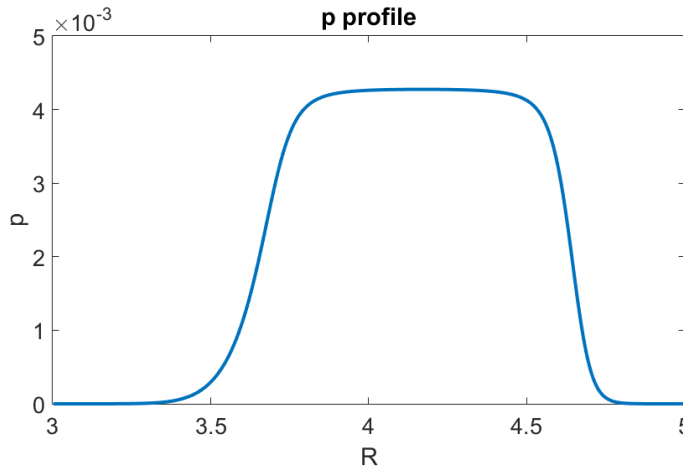
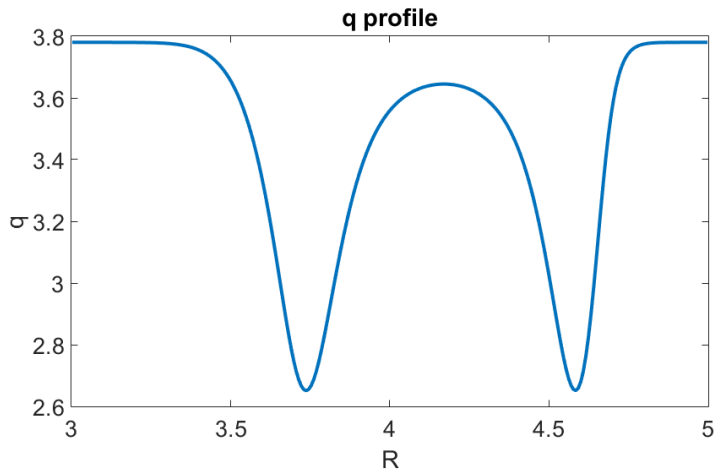


FIG. 7. Linear growth rate as a function of diamagnetic frequency for different values of Lundquist number. With no scaling of ω_* (left). Scaling $\omega^* \propto \eta^{3/5}$ is used (right).



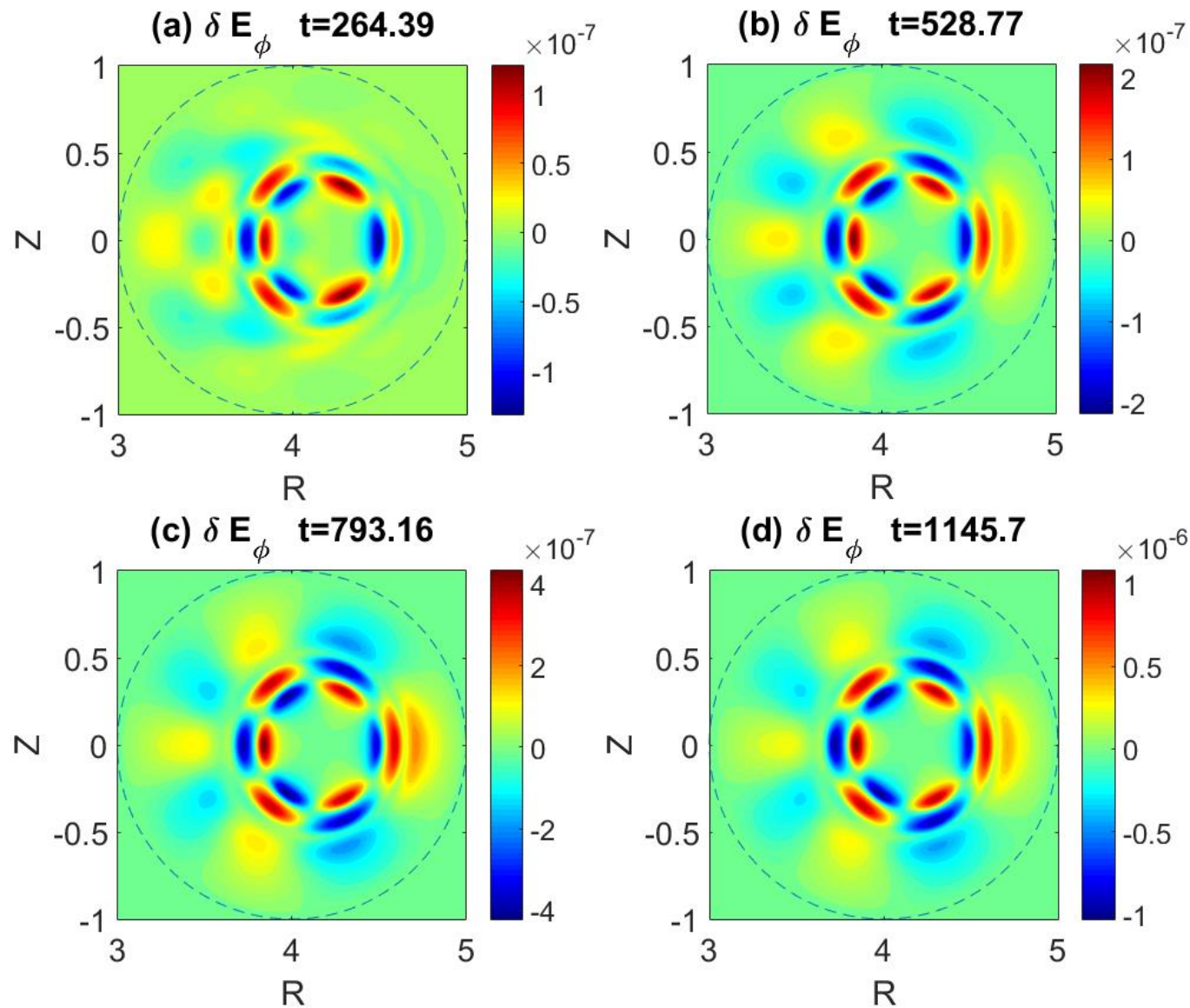
Meshcheriakov, PoP, 2012

3.2 Rotation effect on dynamics of double tearing mode

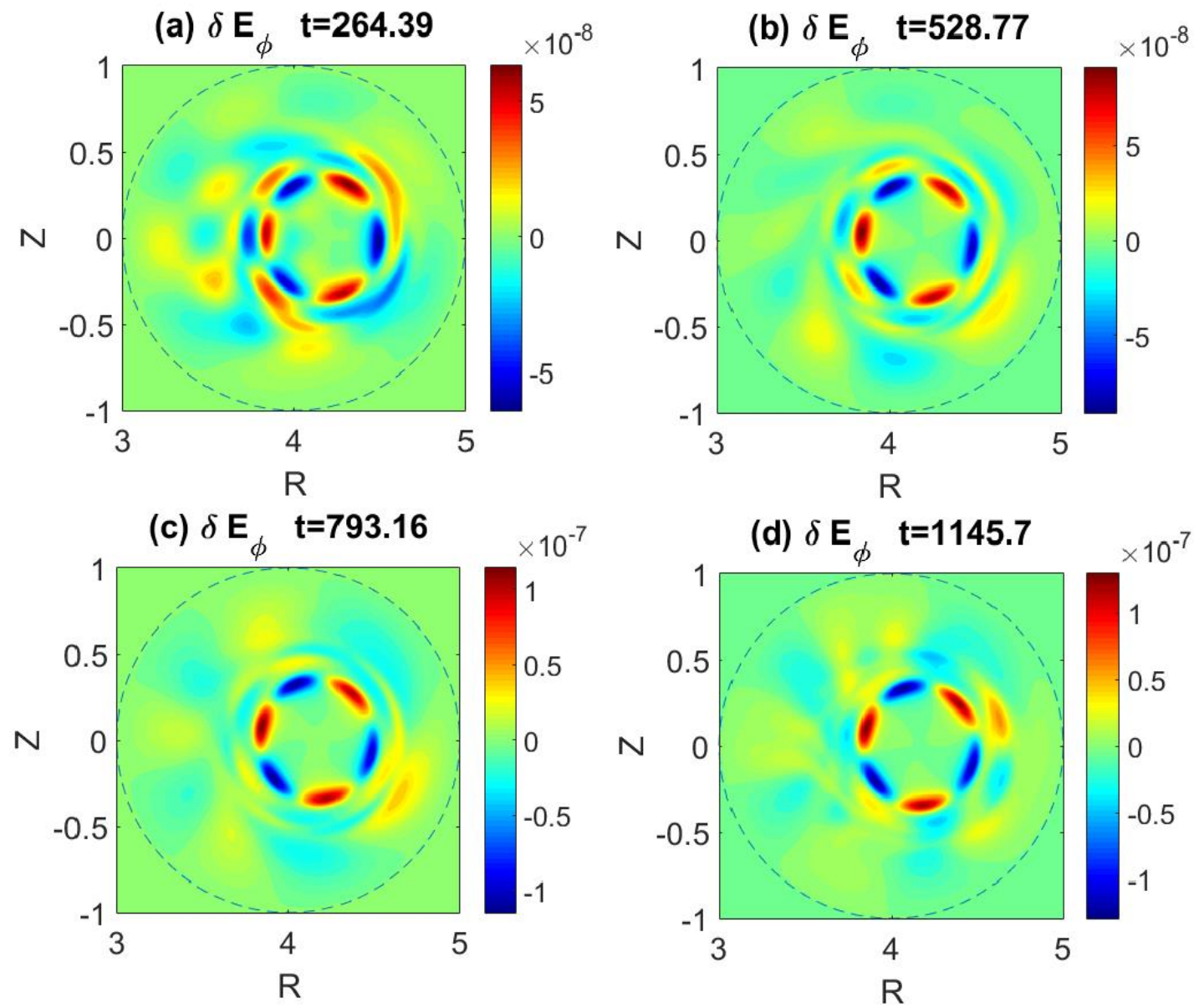


**Kinetic energy
for double Tearing mode**

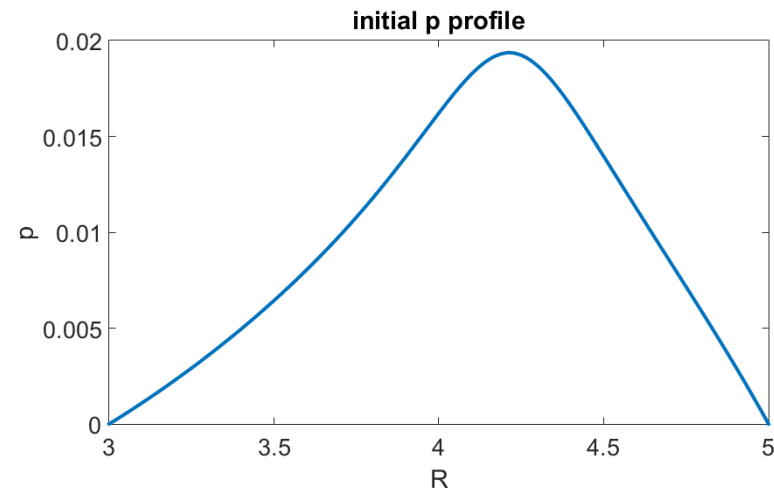
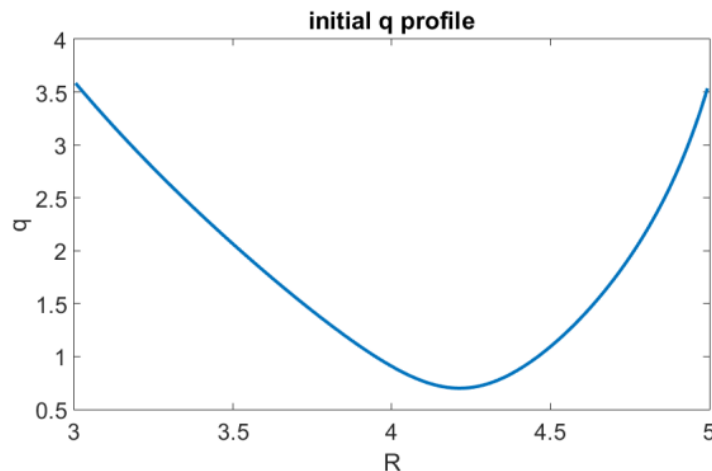
$m/n=3/1$ mode structures without Hall effect



$m/n=3/1$ mode structures with Hall effect

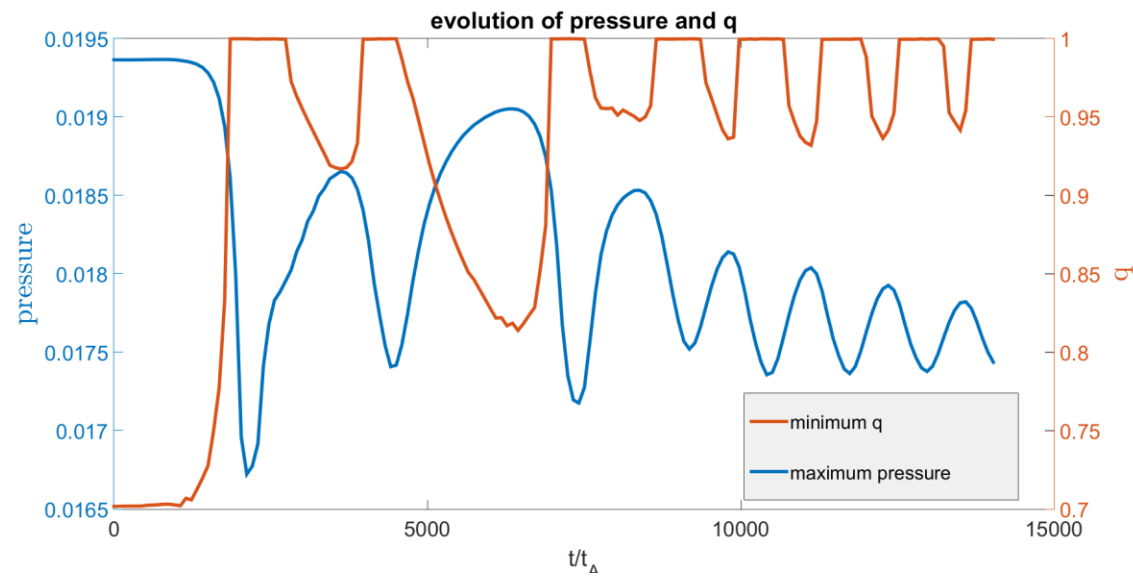


3. Hall effects on sawtooth oscillation

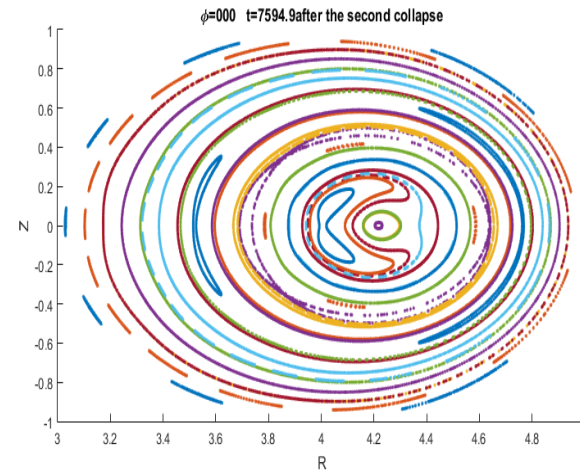
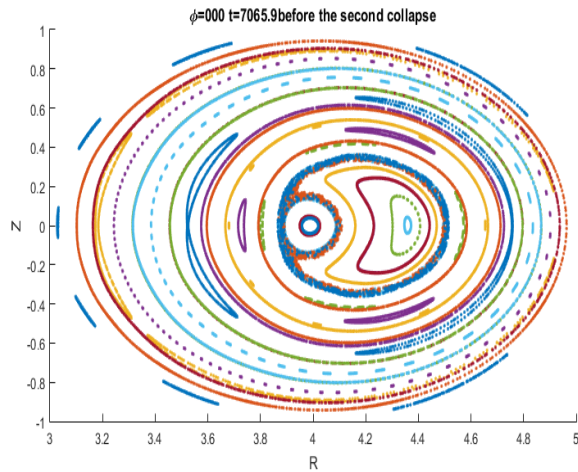
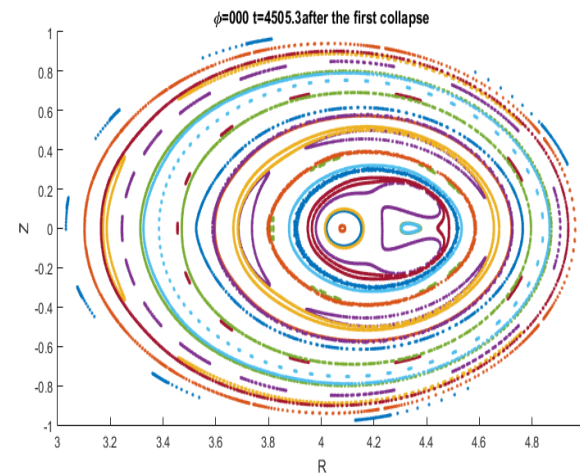
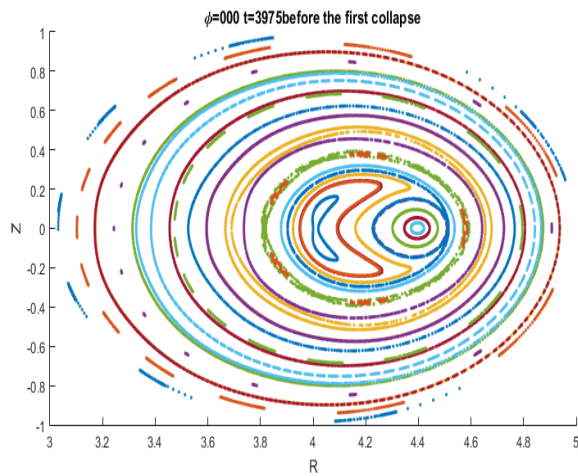


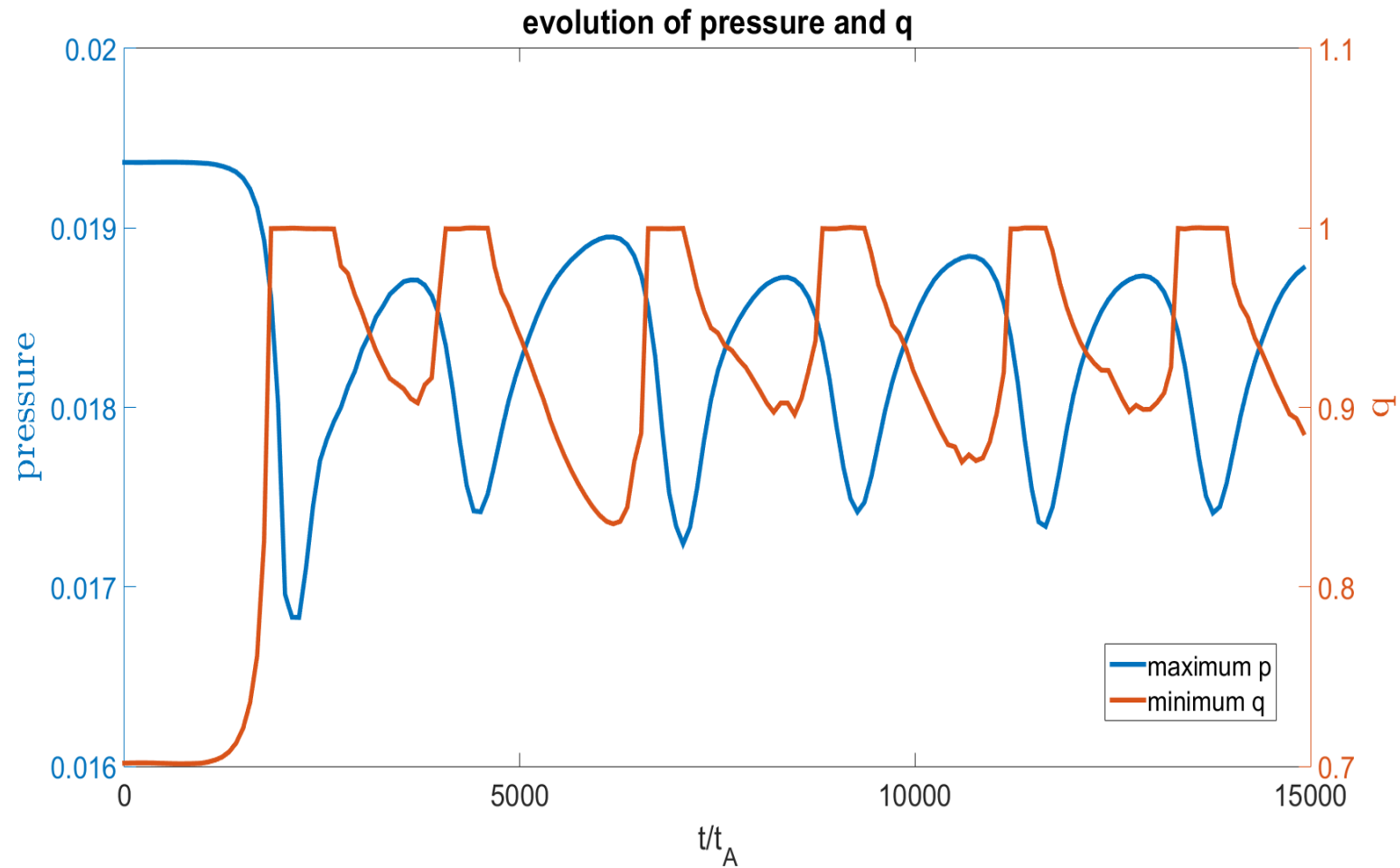
Initial q and pressure profile

Without Hall



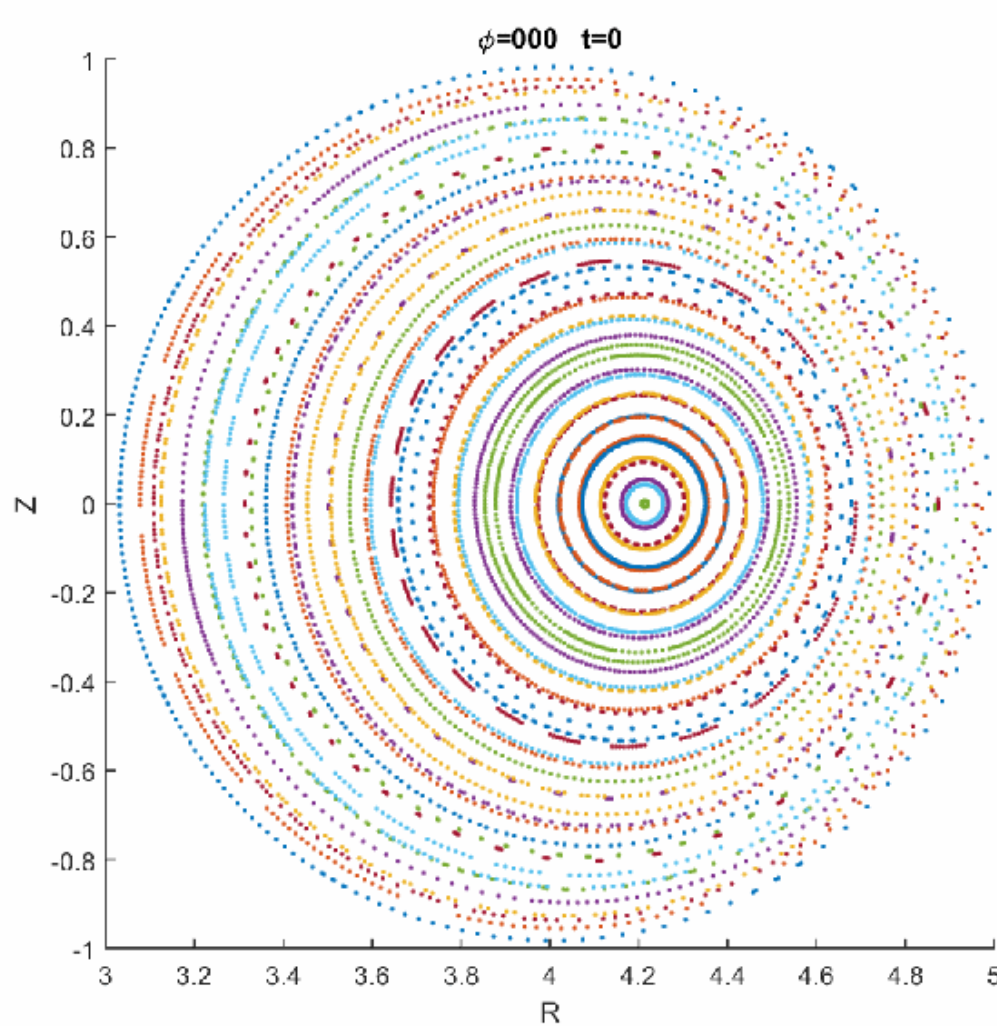
Snapshots of the magnetic flux surfaces





With Hall effects

Snapshots of the magnetic flux surfaces

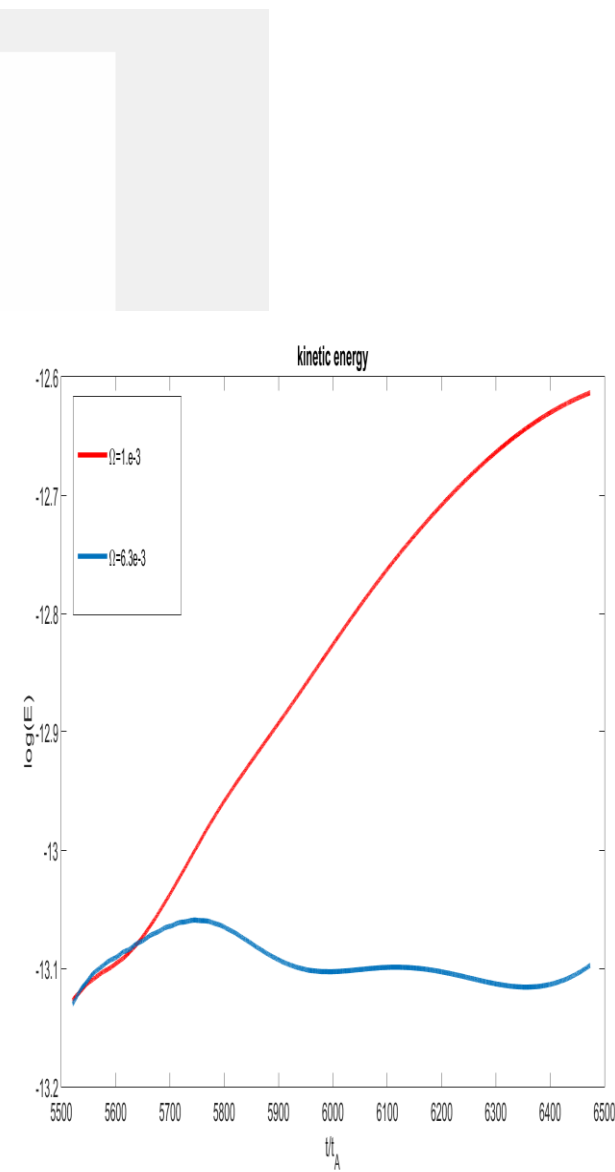
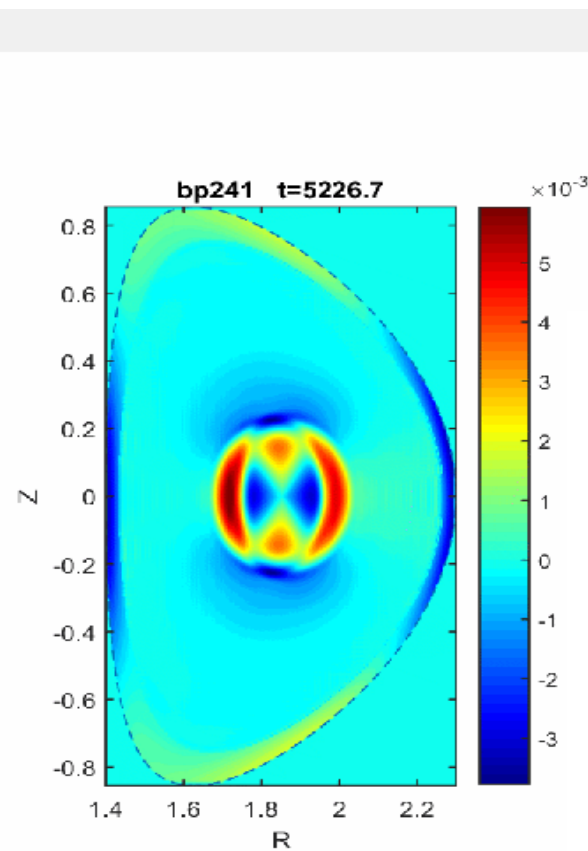
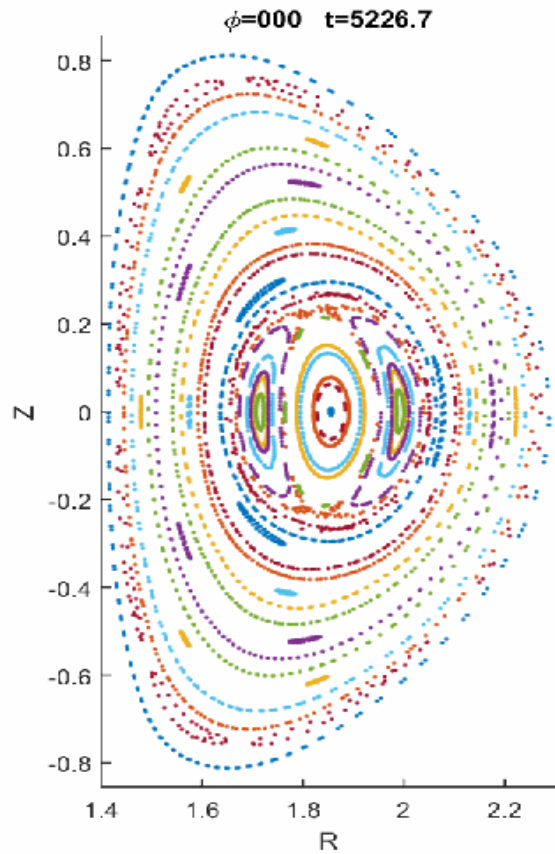


4. Brief Summary

- 1. Tearing mode can effectively controlled by time-dependent external helical driven current.
- 2. Diamagnetic rotation of mode structure without plasma rotation is self-consistently contained in Hall MHD. Linear growth rate increases with increase of ion inertial length.
- 3. Double tearing mode in a reversed shear q profile may not be excited strongly due to diamagnetic rotation in Hall MHD.
- 4. Sawtooth oscillation goes on continuously in Hall MHD while sawtooth oscillation stops after a few of cycles in resistive MHD.

Future research plans:

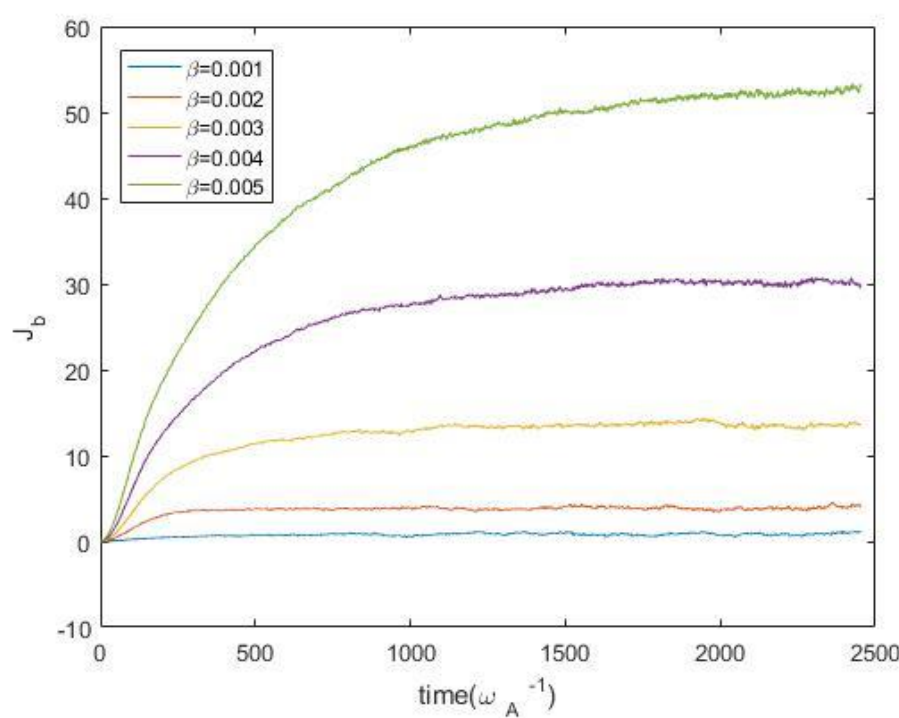
1. Preliminary results for RMP



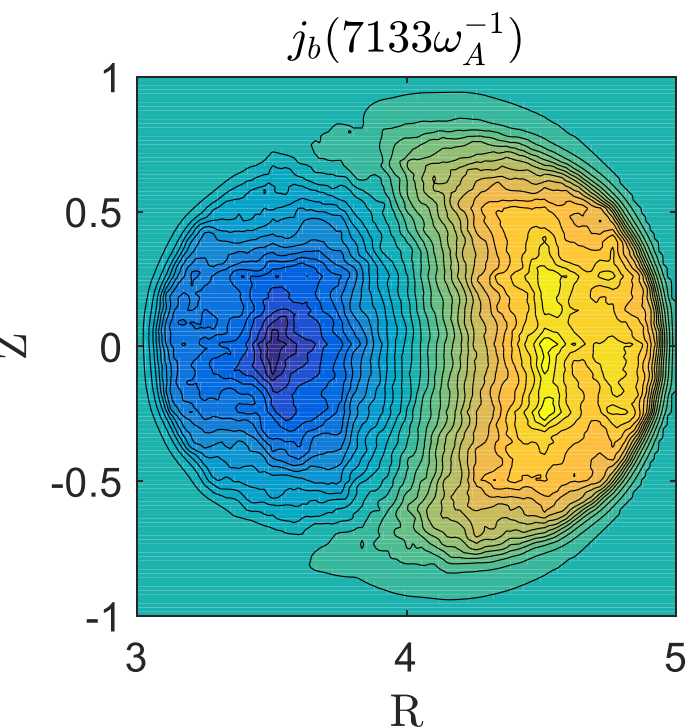
2. Neoclassical tearing mode

Bootstrap Current from CLT-K

J_b with different collision frequencies



J_b distribution



Bootstrap current dependence on collision frequency

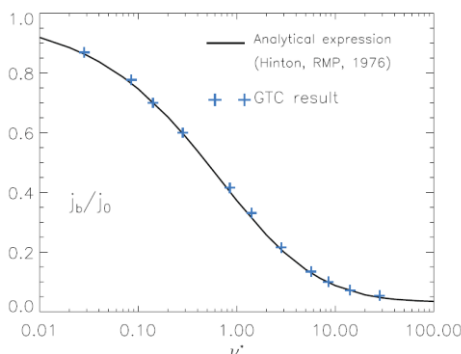
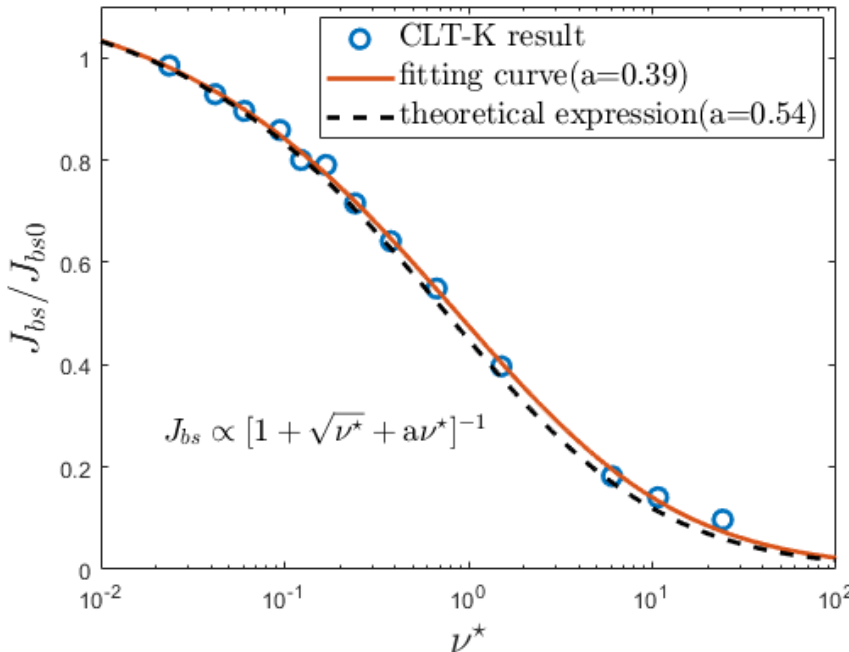


Figure 1. Bootstrap current j_b dependence on collision frequency ν^* without magnetic islands. The solid line is the analytic expression in [3].

Dong NF 2017

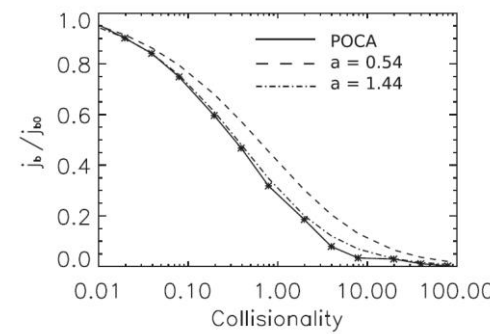


FIG. 5. Scaling of normalized bootstrap current as a function of collisionality. Plotted bootstrap currents are normalized to the bootstrap current at the low collisionality where $\leq 10^{-3}$. POCA calculation shows a good agreement with a theoretical prediction (dashed) and a scaling from another of code (dash-dotted).

Kim, POP 2012

Key points:

1. Every point should be normalized by its collisionless limit
2. For small collision, longer time is needed to reach the steady state.

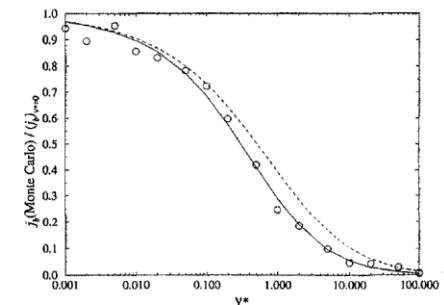


FIG. 4. Normalized bootstrap current vs. collisionality at $\epsilon = 0.1$. The circles represent values obtained from Monte Carlo simulations. The dotted line is the theoretical prediction given by Hinton and Rosenbluth¹ ($j_b \propto [1 + \sqrt{\nu_*} + 0.54\nu_*]^{-1}$) and the solid curve represents a fit where $j_b \propto [1 + \sqrt{\nu_*} + 1.44\nu_*]^{-1}$.

Sasinowski, POP 1995

*Thanks for
your attention!!!*